



Project report

HD-TEG

31 December 2020

**Deutsches Zentrum für Luft-
und Raumfahrt e.V.**

Institute of Vehicle Concepts



HDTEG

Thermoelektrischer Generator im Nutzfahrzeug



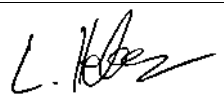
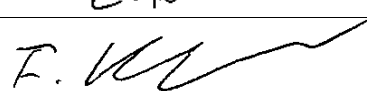
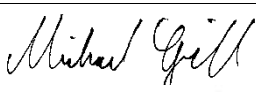
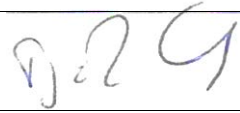

Deutsches Zentrum für Luft- und Raumfahrt e.V.

Institute of Vehicle Concepts
Pfaffenwaldring 38-40
D-70569 Stuttgart, Germany

Institute management
Prof. Dr.-Ing. Tjark Siefkes
Tel.: +49 (0)711/6862-691
FAX.: +49 (0)711/6862-258

Project management
Lars Heber
Tel.: +49 (0)711/6862-8207
FAX.: +49 (0)711/6862-258

Title	HD-TEG		
Author	Lars Heber Tel.: +49 (0)711/6862-8207 lars.heber@dlr.de Other authors: J. Schwab, T. Knobelspies, Dr. M. Grill, K. Yang		
Project	HD-TEG: Potential for increasing the efficiency of heavy duty vehicles through the use of a new type of waste heat recovery system (thermoelectrics)		
File name	2020-12-31_Projektbericht_HD-TEG_V1_[engl].pdf		
File	https://elib.dlr.de/142027/		
Version no.	Amendment	Number of pages	Date
1	Final report_V1	72	31 Dec. 2020

Created		31/03/2021 Lars Heber, Project manager (DLR FK)
Checked		30/04/2021 Dr. F. Rinderknecht, Department manager (DLR FK)
Checked		14/04/2021, Dr. M. Grill Manager 0D/1D-Simulation (FKFS)
Released		30/04/2021, Prof. Dr.-Ing. Tjark Siefkes, Institute manager (DLR FK)
Released		14/04/2021, Dr. M. Grill Manager 0D/1D-Simulation (FKFS)

Translation from the original German version. In case of ambiguity, see original version.

Table of contents

0	Abstract	1
1	Introduction and objective	2
2	Project content and results	4
2.0	WP 0: Project Management & Reporting.....	4
2.1	WP 1: Research on the state of the art of thermoelectrics.....	6
2.2	WP 2: Boundary conditions.....	9
2.3	WP 3: Simulative overall system interactions.....	15
2.3.1	Engine and exhaust gas aftertreatment.....	15
2.3.2	Engine cooling.....	19
2.4	WP 4: Constructive TEG design.....	25
2.4.1	Methodical concept and solution finding.....	25
2.4.2	Validation study.....	25
2.4.3	Dimensioning.....	27
2.4.4	Results of the design process.....	29
2.5	WP 5: overall systemic TEG simulation.....	34
2.5.1	Vehicle interactions.....	34
2.5.2	Techno-economic boundary conditions.....	37
2.5.3	Simulation environments and modeling.....	38
2.5.4	Simulation results.....	43
2.6	WP 6: Validation through functional models.....	47
2.7	WP 7: Evaluation and outlook.....	51
2.7.1	TEG potential assessment and outlook.....	51
2.7.2	Outlook of future HDV engines with regard to waste heat utilization...51	
3	Reflection	55
4	Bibliography	57
5	Appendix	59
5.1	Equations.....	59
5.2	Additional results.....	61

List of figures

Figure 2-1 Structure plan of the HD-TEG project	4
Figure 2-2 Potential analysis of the available exhaust gas temperatures along the exhaust gas system, mass flow as well as backpressure of the exhaust system without TEG in the engine map (output data of the interpolation are based on dynamic simulation values) ...	11
Figure 2-3 Potential analysis based on the available heat flows $Q_{Ex, EGA}$ at the exhaust gas aftertreatment (EGA) outlet in the engine map.	12
Figure 2-4 Detailed images of the vehicle and installation space assessment in the area of the exhaust system of the IVECO Stralis NP460 LNG	14
Figure 2-5 Simulation results for fuel consumption and raw emissions as a function of engine speed and engine torque.....	17
Figure 2-6 Design of the adapted cooling system for Cursor 13 gas engine.....	20
Figure 2-7 Heat balance map as a function of engine speed and torque from simulation results with the air and fuel path model. Left: Absolute heat input into the coolant in kW; Right: Percentage heat input into the coolant in relation to fuel output in %	21
Figure 2-8 Simulation results for cooling potentials of the cooling system when the TEG is connected after the HT cooler with coolant temperature at the engine outlet of 91 °C as the target value at the different driving speeds under ambient temperature of 20 °C	23
Figure 2-9 Maximum permissible heat dissipation of the TEG into the cooling system during constant driving on the level in the HDV with Cursor 13 gas engine for different integration positions of the TEG (12th gear, vehicle mass with 40 t payload, ambient temperature 20 °C)	24
Figure 2-10 Schematic representation of a pure co-current (a) or pure countercurrent heat exchanger (b) as well as fluid flows along the heat exchangers with different heat exchanger surfaces A ((c), (d), boundary conditions: $\vartheta_1' = 600\text{ °C}$, $m_1 = 350\text{ kg/h}$, $\vartheta_2' = 85\text{ °C}$, $m_2 = 10\text{ l/min}$)	30
Figure 2-11 CAD model of the 3-channel TEG result design as a functional model for experimental validation (a) and with transparent housing components (b)	31
Figure 2-12 Design of the test rig structure	32
Figure 2-13 3D CAD model of the TEG installation concept in the exhaust system (colored red) of the reference vehicle of the natural gas tractor unit	33
Figure 2-14 TEG as a subsystem in the overall vehicle system and its interactions	34
Figure 2-15 Resultant change in fuel consumption when the exhaust gas backpressure of the exhaust gas system of the reference vehicle is changed with varying engine output..	35
Figure 2-16 Illustration of the on-board electrical system of a conventional HDV with 24-volt on-board electrical system architecture.....	36
Figure 2-17 Example evaluation of the positive and negative effects of TEG integration in a natural gas HDV in terms of the change in fuel consumption (*for typical load points of highway travel; $B_e = 32.2\text{ kg/100 km}$; specific CO ₂ emissions $c = 813\text{ g/km}$; TEG fully supplies the on-board electrical system)	37

Figure 2-18 TCO cost structure for semitrailer truck with natural gas combustion engine (LNG) with kilometrage of 150,000 km/year (a) and target cost analysis of an example TEG design and indication of its benefit threshold (b; assumptions: Useful life of 5 years for the tractor unit or 10 years for the trailer, $B_s = 35.3$ l/100 km for the diesel or $B_e = 32.2$ kg/100 km or the natural gas HDV, TEG unit cost $K_{TEG} = 1500$ EUR).....38

Figure 2-19 Integration of the CadNexus interface for bidirectional communication of the CAD model in CATIA and ANSYS Workbench.....39

Figure 2-20 Example graphical user interface of the simulation environment in Ansys Workbench40

Figure 2-21 Example transformation from the physical replica using the simulation result via derivation into a mathematical model from the simulative results.....41

Figure 2-22 Module characteristics based on the module measured values of efficiency and electrical power of the selected TEM (LGC100)42

Figure 2-23 Schematic diagram of the CFD model of the model environment.....42

Figure 2-24 Results of the preliminary investigation on the influence of the TEG length in the flow direction.....44

Figure 2-25 TEG functional model as hardware realization of the TEG result design with minimum TCO objective: (a) HDTEG1: Setup with spare modules and (b) HDTEG2: Setup with TEM LGC100 from LG Chem47

Figure 2-26 Schematic diagram of the TEG functional pattern in counterflow design based on the TEG core (without housing components) and the hot gas and coolant flow paths .48

Figure 2-27 Comparison of the hot and cold side temperatures between the simulation and the experiment of the functional model HDTEG2 on the hot gas test rig at operating points 1.1* and 3.2** (*: For boundary conditions, see Table 2-12).....50

Figure 2-28 Breakdown of primary energy used in the internal combustion engine [12] ...52

Figure 2-29 Semitrailer on *Long Haul Cycle*, individual measures [10].....53

Figure 2-30 Change in vehicle costs of a 40 t semitrailer in long-distance transport by 2018 [10]54

Figure 5-1 Result of the potential analysis based on the engine power and the available exhaust enthalpy in the EGA for the natural gas HDV in the WHVC with 15 t TW61

Figure 5-2 Result of the potential analysis based on the engine power and the available exhaust enthalpy in the EGA for the natural gas HDV in the WHVC with 40 t TW61

Figure 5-3 Full load curve of the Cursor 13 gas engine.....62

Figure 5-4 Simulation results for exhaust gas temperatures and mass flows, IK value, pressure losses in the three-way catalytic converter as a function of engine speed and torque63

Figure 5-5 WHSC operating points64

Figure 5-6 Simulation results for specific fuel consumption and exhaust emissions in WHSC operating points64

Figure 5-7 Simulation results for exhaust gas temperatures at different locations in the exhaust line of the Cursor 13 gas engine.....65

Figure 5-8 Simulative studies for the influence of additional exhaust gas backpressure on specific fuel consumption at WHSC operating points in OP01-0666

Figure 5-9 Continuation of Figure 5-8 for OP07-1167

Figure 5-10 Fan ratios at the different driving speeds (ambient temperature of 20 °C; dry – 0 % humidity, air pressure of 1.013 bar).....68

Figure 5-11 Simulation results for cooling potentials of the cooling system when the TEG is connected after the HT cooler with coolant temperature at the engine outlet of 100 °C as the target value at the different driving speeds under ambient temperature of 20 °C69

Figure 5-12 Simulation results for cooling potentials of the cooling system when the TEG is connected after the intercooler with coolant temperature at the engine outlet of 100 °C as the target value at the different driving speeds under ambient temperature of 20 °C70

Figure 5-13 Result of the TEG performance in WHVC with 15 t TW in the result design with target for minimum TCO (TEG system integrated at the outlet of the EGA and in the LT CC)71

Figure 5-14 Result of the TEG performance in WHVC with 40 t TW in the result design with target for minimum TCO (TEG system integrated at the outlet of the EGA and in the LT CC)71

Figure 5-15 HDTEG2 functional model on DLR's own hot gas test rig72

List of tables

Table 2-1 Milestone overview of the project and indication of the respective status as of 31 December 2020 (adjustment during the course of the project)	4
Table 2-2 Overview of the technology-relevant properties of major thermoelectric material classes, representation based on [4].....	7
Table 2-3 Overview of the state of the art of TEG research for HCV	8
Table 2-4 Market overview of natural gas HDV for regional and long-distance traffic.....	9
Table 2-5 Carnot efficiency η_c and triangular process efficiency η_{Dr} for different heat sources ϑ_h and heatsinks ϑ_c in the natural gas HDV	10
Table 2-6 Overview of the defined operating points (OP) for the TEG design	13
Table 2-7 Overview of conventional TEG configurations, figures from [7]	25
Table 2-8 Results of the preliminary investigation with commercial TEMs based on the preliminary study.....	27
Table 2-9 Dimensioning the number of TEG stacks	28
Table 2-10 Overview based on the manufacturer's data of the investigated highly efficient and segmented TEM for high operating temperatures of LG Chem Ltd.....	41
Table 2-11 Result of the optimization of holistic TEG system design (TEG result design selected for maximum reduction of fuel consumption at most favorable system cost balanced over all operating points, OP)	46
Table 2-12 Comparison of the average hot ϑ_{HS} and cold side temperatures ϑ_{CS} as well as the electrical generator output P_{TEG} between the simulation and the experiment of the HDTEG2 functional model on the hot gas test rig	49
Table 5-1 Technical data of the research engine, Cursor 13 gas engine.....	62
Table 5-2 WHSC operating points.....	64
Table 5-3 HDV data for the simulation	70
Table 5-4 Comparison of the hot gas backpressure Δp_{TEG} between the simulation and the experiments of the HDTEG1 and HDTEG2 functional models on the hot gas test rig.....	72

List of abbreviations

CC	Coolant circuit
CO ₂	Carbon dioxide
COHEX	Coolant heat exchanger
DLR FK	Deutsches Zentrum für Luft- und Raumfahrt (DLR e.V.) (German Aerospace Center, Institute of Vehicle Concepts)
e.g.	for example
EGA	Exhaust gas aftertreatment
EGR	Exhaust gas recirculation
EU	European Union
FKFS	Forschungsinstitut für Kraftfahrwesen und Fahrzeugmotoren Stuttgart
GT	Gamma Technologies
HCV	Heavy-duty commercial vehicle
HDV	Heavy-duty vehicle
HEX	Heat exchanger
HGHEX	Hot gas heat exchanger
HT	High temperature
i.e.	that is
LNG	Liquefied natural gas
LT	Low temperature
MS	Milestone
n.a.	not applicable
NO _x	Nitrogen oxides
OP	Operating point
SHHS	Stuttgart – Hamburg – Stuttgart (reference route)
TCO	Total Cost of Ownership
TEG	Thermoelectric generator
TEM	Thermoelectric module
TW	Total weight
WHSC	World Harmonized Stationary Cycle
WHTC	World Harmonized Transient Cycle
WHVC	World Harmonized Vehicle Cycle
WP	Work package

0 Abstract

In this project, the improvement in efficiency of modern heavy-duty commercial vehicles was demonstrated through the use of a new type of waste heat recovery system. For the first time, a heavy-duty vehicle-specific system based on thermoelectrics was developed using a holistic development approach and the potential of this technology for current and future heavy-duty vehicles was demonstrated. The reference vehicle was an innovative series-produced heavy-duty vehicle with a natural gas engine that is regarded as a key technology for future low-emission road haulage in both the short-haul and long-haul sectors.

The project focused equally on increasing the efficiency of the thermoelectric system and the vehicle as well as on reducing the cost of the system by using near-series assembly technologies and manufacturing processes. The system costs of waste heat recovery systems in heavy-duty vehicles must be amortized in real operation in the shortest possible time, depending on the application. A design of the TEG was chosen for this that promises a high energy yield combined with low weight at the same time, thus offering advantages both under real driving conditions and in relevant driving cycles. A new type of holistic design method offers the potential of designing thermoelectric systems much more efficiently in the future. Apart from the system design, all interactions with the heavy-duty vehicle were also considered and quantified for the first time. The implementation of these approaches was presented in several functional models. Thanks to close cooperation between the project partners, the knowledge and extensive experience of both were able to flow into the project to help the technology achieve a breakthrough in heavy-duty vehicles.

As a result, a waste heat recovery system in the form of a thermoelectric generator for an innovative natural gas heavy-duty vehicle was designed economically for the first time. The calculated amortization was mostly achieved in a period of less than two years, assuming series development of the system. Depending on the driving scenario and the load points, this is already within the realm of possibility after one year. The fuel reduction is up to 2.5 %, equivalent to 1 kg/100 km of fuel. Future potential is a further 1.2 percentage points. In a hardware implementation, more than 2.5 kW of electrical power was measured on the functional model.

1 Introduction and objective

To further reduce exhaust gas emissions (especially CO₂ emissions) as well as the energy consumption of a heavy-duty vehicle (HDV), the internal engine measures focused on in research and development to date are not sufficient on their own. Modern heavy-duty vehicle engines are expected to meet the highest standards in terms of economy, especially fuel consumption and investment costs, as well as pollutant emissions. As a result of the high level of technological development of the diesel internal combustion engines used almost exclusively today in the heavy-duty commercial vehicle (HCV) sector, further optimization is becoming increasingly difficult in terms of the decisive cost-benefit ratio. Therefore, alternative development paths must be considered for the further optimization of vehicles, which include component development in the context of the entire vehicle and develop it with regard to the aforementioned cost-benefit ratio. In addition, aspects such as alternative drive concepts and fuels as well as the increasing electrification of auxiliary units are worth mentioning and taking into account.

In the case of HDVs, operators focus primarily on the total cost of ownership (TCO). Fuel consumption is an immense cost factor for the freight forwarder's ongoing operating costs whereas low emissions are essential for manufacturers to meet regulatory requirements. In the past, manufacturers focused mainly on reducing emissions of nitrogen oxides (NO_x). In the future, CO₂ emissions, and, hence, fuel consumption, will become much more important. According to the only publicly available source on consumption data of heavy-duty vehicles on a test track in the magazine Lastauto Omnibus, the consumption of HCVs has not decreased significantly over the last 25 years [1]. New possibilities for reducing consumption must therefore be increasingly considered. One promising approach is a waste heat recovery system to increase vehicle efficiency, for example, and thus reduce consumption and exhaust gas emissions.

The use of gaseous fuels such as natural gas offers great potential for reducing CO₂ due to its chemical composition. This is in the range of around 25% compared to conventional fuels, due to the better carbon to hydrogen ratio. So far, gas engines cannot be operated with the same high efficiency as conventional diesel engines – but current national and international research projects show promising approaches. This project also increases the attractiveness of natural gas combustion engine technology through the combination

of an innovative drive and waste heat recovery concept in the form of a thermoelectric generator (TEG) and favors the use of lower-emission drive concepts. This addresses the regulations to be expected in the future, in particular with regard to CO₂ and fuel reduction, and also the development of efficient gas drives as part of the mobility and fuel strategy of the German government [2] as well as the European Union (EU) with the LNG Blue Corridor project (*Liquefied Natural Gas*, LNG) [3].

In the HD-TEG project described here, a TEG application for a series-produced heavy-duty commercial vehicle with a natural gas engine was developed for the first time and tested on the basis of experimental investigations on functional models. This approach provides a sound knowledge base in the field of TEG application and can be useful for future projects and technology understanding in the automotive industry. Close cooperation between the DLR FK facilities and the FKFS allows expertise in the development of waste heat recovery systems and engine technology expertise to be used synergetically. A comprehensive investigation of TEG technology for heavy-duty vehicles was carried out for the first time, which is to fulfill both technical and economic constraints using a specific and specially developed heavy-duty vehicle development method. Neither a validation of the potential estimates (at vehicle level) nor a development specific to heavy-duty vehicles in the context of the entire vehicle has been carried out so far. Thanks to the competence of the project partners and the significantly increased power densities of TEG systems by DLR FK, this gap in the research was addressed with the help of the knowledge gained in order to make reliable statements about the potential of TEG systems in heavy-duty vehicle applications.

2 Project content and results

2.0 WP 0: Project Management & Reporting

The project comprises 7 work packages (WP) that are presented in Figure 2-1 as an overview. The responsible organizational unit is identified by its logo.

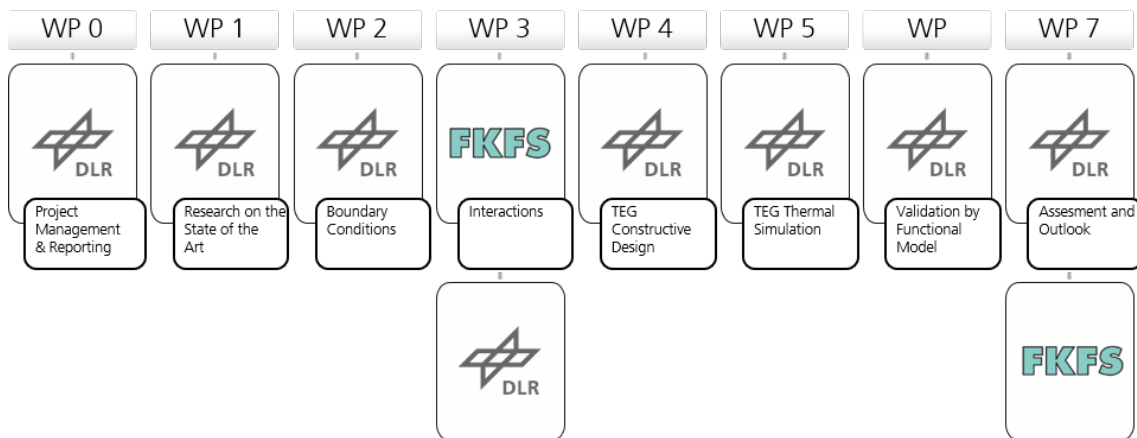


Figure 2-1 Structure plan of the HD-TEG project

In the project, as shown in Table 2-1, all milestones were met and it was successfully completed with outstanding results.

Table 2-1 Milestone overview of the project and indication of the respective status as of 31 December 2020 (adjustment during the course of the project)

Mile-stone (MS)	Due date	Institute	Designation	Status
MS 0	03/2018	DLR-FK	Kick-off meeting	Completed.
MS 1	11/2019	DLR-FK	(Simulation) Results for reference vehicle are present	Completed.
MS 2	02/2020	FKFS	Total system interactions are present	Completed.
MS 3	03/2020	DLR-FK	TEG design is complete	Completed.
MS 4	11/2020	DLR-FK	TEG functional model is built	Completed.
MS 5	12/2020	DLR-FK	Measurement results from the TEG functional model are present	Completed.
MS 6	12/2020	DLR-FK	Completion of the project on the basis of the final report	Completed.

In the course of the project so far, the following publications have been made:

- Heber, Lars (2018): *Thermoelectric Generators for Heavy-Duty Vehicles: A Systemic Approach and Development*. ICT/ECT-2018, 02.-05. Jul. 2018, Caen, France.
- Heber, Lars; Schwab, Julian and Friedrich, Horst E. (2018): *Design of a Thermoelectric Generator for Heavy-Duty Vehicles: Approach Based on WHVC and Real Driving Vehicle Boundary Conditions*. Springer Nature Scientific Publishing Services (P) Ltd., 2. ETA-Tagung | Energie- und Thermomanagement, Klimatisierung, Abwärmenutzung (ETA Conference | Energy and Thermal Management, Air Conditioning, Waste Heat Utilization), 22. - 23. Nov. 2018, Berlin, Germany.
- Heber, Lars; Schwab, Julian; Yang, Kangyi and Grill, Michael (2019): *Effects of a Thermoelectric Waste Heat Recovery System on the Engine Performance and the Cooling System of a Natural Gas Powered Heavy-Duty Vehicle*. 5th Annual World Congress of Smart Materials 2019, 06.-08. March 2019, Rome, Italy.
- Heber, Lars and Schwab, Julian (2019): *Thermoelectric Generators in Heavy-Duty Vehicle Applications: Development Approach and Optimization under Real Driving Conditions*. ICT/ACT 2019 - International Conference on Thermoelectrics, 30. June - 04. July 2019, Gyeongju, Korea.
- Heber, Lars and Schwab, Julian (2020): *Modelling of a thermoelectric generator for heavy-duty natural gas vehicles: Techno-economic approach and experimental investigation*. Applied Thermal Engineering, 174 (11515). Elsevier.

2.1 WP 1: Research on the state of the art of thermoelectrics

This work package included research conducted on the state of the art regarding thermoelectrics and, specifically, the development of TEG for the HDV application, which is useful for ranking against alternative waste heat recovery systems. The data basis is based on a literature review, participation in specialist conferences and conducting expert interviews.

The technology-relevant material classes for thermoelectric modules (TEM) in TEG are listed and their use in the HCV is evaluated in Table 2-2. The areas marked in red represent critical material properties that make their use in heavy-duty vehicles difficult or impossible. For low temperature applications, bismuth telluride (BiTe) TEMs are currently the best alternative due to availability, efficiency and reliability. For high-temperature applications, the material classes of skutterudites and half-Heusler alloys represent the most favorable selection at the moment. The development maturity of the two classes of high-temperature materials is not yet comparable to BiTe-TEM, however, which has been researched for some time. In general, module costs must be taken into account when selecting materials for the overall system design, e.g. by reducing the amount of material used per module or the number of modules.

An overview of previous work and research activities in the field of thermoelectrics for HCV and their results can be found in Table 2-3. Noticeable and worth highlighting are the numerous fields marked in red where no information (n.a.) is available for the TEG projects. Information on construction methods and gross outputs of TEG systems is extensively available, but specific findings or data regarding efficiency, TEG weight, boundary conditions, system costs, and fuel economy, for example, are lacking, reflecting the state of development of TEG technology in the HCV application area. Until now, there has been a lack of a scientifically comprehensible overall system design to conclude the (net) fuel savings as well as the costs and the amortization period of the systems from the gross performance of the systems. Due to the gap in research, it is not possible to compare or evaluate the projects carried out.

Table 2-2 Overview of the technology-relevant properties of major thermoelectric material classes, representation based on [4]

Material Classification	Bismuth Telluride	Bismuth Antimonide	Lead Telluride	TAGS	Skutterudite	Zintl Phase	Iron Silicide	Magnesium Silicide	Higher Magnesium Silicide	Zinc Antimonide	Half-Heusters	Silicon / SiGe	Clathrate	Oxide
Basis Material	BiTe	Bi-Sb	PbTe / Ag _{1-x} Pb _x SbTe _{2-xm}	(AgSbTe ₂) _{1-x} (GaTe) _x	R ₂ CoSb ₂	various	FeS ₂	Mg ₂ Si	Mg ₂ Sn _{1-x} Si _{1+x}	Zn ₄ Sb ₃	various	Si / SiGe	various	various
Operable Temperature Range [K]	< 500 K	< 300 K	300 - 800 K	500 - 900 K	300 - 900 K	500 - 1100 K	500 - 1200 K	300 - 900 K	300 - 900 K	250 - 670 K	300 - 1000 K	600 - 1300 K	> 600 K	> 800 K
Max. ZT p/n	1,4 / 1,0	-0,3	1,8 / 1,3	1,5	1,0 / 1,7	-1,0	0,2 / 0,4	0,5 - 1,1	0,6 - 0,8	1,0 (p only)	0,8	0,1 - 0,7	0,6 / 1,4	0,2 - 1,0
At Temperature (Ca.)	430 K	200 K	750 K	750 K	750 K	> 700 K	900 K	800 K	800 K	650 K	700 - 1000 K	800 - 1300 K	800 - 1000 K	1000 K
Thermal Stability	bis 250 °C	k. A.	oxidation protection necessary	unstable	OK, oxidation protection necessary	unstable	yes	not clear, oxidation protection necessary	unstable	unstable in air, degradation	OK	OK	OK	OK
Contacting Developed	OK	OK	OK	OK	under development	no	under development	OK	no	OK	OK	OK	unknown	under development
Commodity Price (\$/kg) *	190	20	60 - 200	varies widely	16 + x	strongly dependent on YB content	3	4 - 20	4 + x	10	25 - 250	3 (Si) 150 - 420 (SiGe)	1000	ab 30
Potential Suppliers	various	unknown	unknown	unknown	Tegma, Trebacher	unknown	NST	Romny, Komatsu	unknown	(AlpCon)	GMZ	unknown	unknown	unknown
Critical Elements, Price	Te	--	Ag, Te	Ge, Ag	Yb, Ca, In	Yb	--	(Ge)	(Ge)	--	Hf	Ge	Ge, Yb	--
Environmental Compatibility	not clear	not clear	lead	not clear	OK	not clear	OK	OK	OK	OK	not clear	OK	not clear	not clear
Field of Application	diesel heavy-duty vehicle	not clear	diesel heavy-duty vehicle	diesel heavy-duty vehicle	natural gas heavy-duty vehicle	natural gas heavy-duty vehicle	not clear	diesel/natural gas heavy-duty vehicle	diesel/natural gas heavy-duty vehicle	not clear	natural gas heavy-duty vehicle	not clear	not clear	not clear

Table 2-3 Overview of the state of the art of TEG research for HCV

(Abbreviations: EM: Exhaust manifold; EGA: Exhaust gas aftertreatment; EGR: Exhaust gas recirculation; N3: EU vehicle class category; vKat: before catalytic converter)

Jahr	TEG System (company name or project name)	Reference System	Technological Maturity	Layout / Topologie HX	Layout / Material TEM	Maximum TEG Power	Ø TEG Power	TEG Net Efficiency	TEG Weight, Volume	TEG Power Density	Exhaust Mass Flow	Exhaust Temperature	Coolant Temperature	Design Method (Simulation)	System Costs	Fuel Saving	Source
						Pe,max (kW)	Ø Pel (W)	η _{max} (%)	M _{TEG} , V _{TEG} (kg/l)	ρ _{TEG} (W/kg; W/l)	m _{Exh} , v _{Exh} (kg/s)	T _{Exh} (°C)	T _{CC} (°C)		K _{TEG} (USD/W)	ABs (%)	
1991-1994 or 2000-2004	Hz-T technology, Inc.	diesel engine (14 L, 250 kW), diesel engine (12 L, 150 kW), diesel engine class N3 (412 kW)	functional model	octagonal design (metal stage inside, air / fins)	flar-plate TEM / BiTe	1000	BCAT: 600 (gross)	N/A	13.6 kg, 10.3 l (TEG-core)	73.5 W/kg or 97.1 W/l (gross, TEG-core)	0.46	627	N/A	experiment	N/A	N/A	Bass und Eisner (1991)
2008	Magna Powertrain Engineering	diesel heavy-duty vehicle class N3 (12 l)	simulation study	stack design	flar-plate TEM / BiTe and SiGe	2700	BCAT: 179, EGA: 982, EGM: 1200 (gross)	TC: 2.1, EGA: 5.4 - 8.5, EM: 5.6 - 9.5,	N/A	N/A	according to cycle	according to cycle	according to cycle	1D-analytic simulation	N/A	0.48 - 0.96	Epleiner et al. (2008)
2005-2011	Michigan State University et al.	diesel engine (151, 403 kW)	laboratory evaluation model	cylindrical design / ribs	flar-plate TEM / SKD, LAST	AGR: 74,7	N/A	2.8 - 6.2	N/A	N/A	0.054 - 0.1	max. 650	52	1D-analytic simulation, experiment	0.93 - 0.45 \$/W (netto)	K.A.	Schock et al. (2011)
2008-2011	RENOTER	diesel heavy-duty vehicle class N3 (111, 338 kW)	simulation study	stack design	flar-plate TEM / BiTe and SiGe	1200	EGR: 100 - 1200 (gross)	N/A	10 kg, 7 l (gross, TEG-core)	120 W/kg or 171.4 W/l (gross, TEG-core)	0.045	400	N/A	2D-analytic simulation	N/A	N/A	Axela (2011)
2013	Magna Powertrain Engineering	diesel heavy-duty vehicle class N3 (70.61, 270 kW, Euro III)	laboratory evaluation model	stack and hexagonal design	TEM Strips / BiTe	200	N/A	5	N/A	N/A	0.25	300 - 400	50 - 100	1D + 3D-CFD simulation, experiment	N/A	N/A	Slener et al. (2013)
2015	Eberspächer Exh. Tech.	diesel heavy-duty vehicle class N3	laboratory evaluation model	stack design	flar-plate TEM / BiTe	AGN: 550	AEGA: 219 (gross)	1.6	N/A	N/A	0.278	350	80	1D + 3D-CFD simulation, experiment	N/A	N/A	Gleiser et al. (2015)
2012-2015	MAN (M. Bernath)	diesel heavy-duty vehicle class N3 (12.4 l, Euro V)	laboratory evaluation model	cylindrical design / ribs	Y-config. / segmented BiTe and SKD (TEG prototype / Euro V)	1200	AEGR: 578 (gross)	N/A	N/A	N/A	according to cycle	according to cycle	LT (Ca. 40) and HT (Ca. 70) CC	1D-analytic simulation, experiment	N/A	0.28 - 0.7	Bernath (2016)
2013-2015	Scania et al.	diesel heavy-duty vehicle class N3 (12.7 l, 446 kW)	prototype in vehicle	stack design	flar-plate TEM / BiTe	785	3EGR+ aECA: 225 (gross), 225 (net)	27 - 5.4	N/A	1.125 W/kg	0.117 - 0.387	aEGA: 248 - 386; EGR: 316 - 360	95 - 100	simulation (1-point-opti., 9-point-vehic. inst.)	150 \$/W (net)	N/A	Risseh et al. (2017)
2014-2017	GASTONE	LNG engine test bench (8.71, 243 kW)	simulation study	round fins	round center hole TEM / SKD	820	506 (gross, simulative)	N/A	N/A	N/A	according to cycle	according to cycle, > 700	N/A	1D-analytic simulation	N/A	N/A	Hervas-Banco et al. (2017)

2.2 WP 2: Boundary conditions

In WP 2, the selection and measurement of an HCV was carried out, which will serve as a representative reference vehicle in the subsequent course of the project. This determined the boundary conditions for the TEG. An overview of the available vehicles can be found in Table 2-4. After reviewing the technical requirements as well as availability, the selection fell in favor of the Iveco Stralis NP, as it was the only production-ready pure natural gas HDV suitable for long-distance transport (≥ 300 kW drive power) at the start of the project. Due to contractual complications, the provision of the vehicles initially led to time delays in the project and could not be carried out as part of this project. Instead, a simulation study was commissioned to determine the vehicle boundary condition.

Table 2-4 Market overview of natural gas HDV for regional and long-distance traffic



Model	Iveco Stralis NP	Mercedes-Benz Econic NGT	SCANIA P/G 340 LNG	Volvo FM LNG	Volvo FH LNG
Fuel	LNG/C-LNG/CNG	CNG	C(B-)NG/LNG	LNG + diesel	LNG + diesel
Engine	Cursor 9/Cursor 13	M 936 G	OC09 /OC13	G13C	G13C
Displacement	8,7 l / 13 l	7,7 l	9,3 l / 12,7 l	13 l	13 l
Maximum Power	294 kW (400 PS) 338 kW (460 PS)	222 kW (302 PS)	250 kW (340 PS) 302 kW (410 PS)	309 kW (420 PS) 338 kW (460 PS)	309 kW (420 PS) 338 kW (460 PS)
Maximum Torque	1700 Nm / 2000 Nm	1200 Nm	1600 Nm / 2000 Nm	2100 Nm / 2300 Nm	2100 Nm/2300 Nm
Total Mass	40 t	32 - 40 t	40 t	40 t	40 t
Maximum Range	1600 km / 1035 km / 570 km	k. A.	500 km / 1600 km	1000 km	1000 km
Emission Standard	Euro VI	Euro VI	Euro VI	Euro VI	Euro VI
Reference	www.iveco.de	www.Daimler.de	www.Scania.de	www.Volvotrucks.de	www.Volvotrucks.de

Several energy sources are available in the HDV for energy recovery. Besides the waste heat utilization, their potential for thermal energy recuperation, i.e. the exergy they contain, plays a significant role. To evaluate the available integration positions and concepts for waste heat recovery in a natural gas HCV, the theoretical efficiency as well as the quality and quantity of the available energy flows are analyzed. This serves as the basis for the TEG design.

Based on the available waste heat sources, the theoretically possible and potential efficiencies of the available energy streams for waste heat utilization in the natural gas HDV are presented in Table 2-5 (see equations (2) and (3) in chapter 5.1 of the Appendix). This clearly shows that the greater the temperature and enthalpy difference, the higher the efficiencies that can be achieved. Waste heat utilization at the engine output offers the highest potential, followed by utilization at the exhaust gas aftertreatment outlet (EGA). One of the project goals was to ensure that the TEG integration had as little impact as possible on the overall vehicle system. The position at the exit of the EGA appeared to be the most reasonable location for the TEG, therefore, and was pursued.

Table 2-5 Carnot efficiency η_c and triangular process efficiency η_{Dr} for different heat sources ϑ_h and heatsinks ϑ_c in the natural gas HDV

Waste heat source	Environment		Low temperature cooling circuit (LT CC)		High temperature cooling circuit (HT CC)		
	ϑ_c	20 °C	60 °C	90 °C			
	ϑ_h	n_c	n_{Dr}	n_c	n_{Dr}	n_c	n_{Dr}
High temperature cooling circuit	90 °C	19.3 %	10.3%	8.3%	4.2%	n.a.	n.a.
Charge air	100 °C	21.4%	11.6%	10.7%	5.6%	2.7%	1.4%
Exhaust gas EGA outlet	670 °C	68.9%	47.3%	64.7%	43.2%	61.5%	40.2%
Exhaust gas engine outlet	800 °C	72.7%	51.2%	69.0%	47.3%	66.2%	44.6%

The following analysis of the relevant boundary conditions of the exhaust gas system for a TEG system in Figure 2-2 and Figure 2-3 is based on the 0D/1D vehicle simulation of the FKFS. Unless specified, the data for the Stuttgart-Hamburg-Stuttgart route (SHHS) serve as the basis. The simulation was commissioned as an alternative to real driving data within the project and serves as a basis for the TEG design by DLR FK.

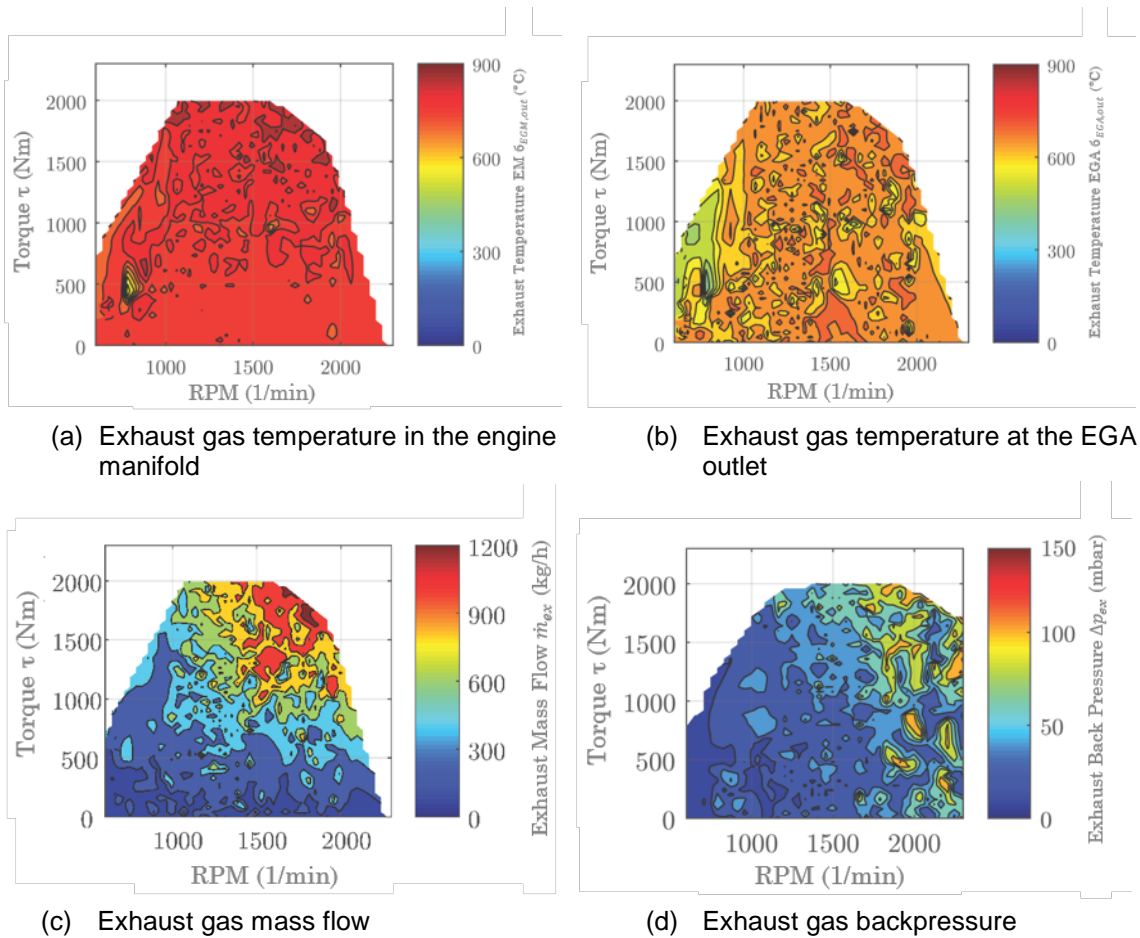


Figure 2-2 Potential analysis of the available exhaust gas temperatures along the exhaust gas system, mass flow as well as backpressure of the exhaust system without TEG in the engine map (output data of the interpolation are based on dynamic simulation values)

From Figure 2-2, it is evident from the inhomogeneous contour surfaces of the three-dimensional polynomial interpolation that a long-distance HDV has non-continuous operating behavior. This makes a TEG design under dynamic boundary conditions appear indispensable. The exhaust gas temperature in the engine manifold (a) is relatively constant, averaging around 800 °C over the entire engine map. The exhaust gas temperature at the outlet of the EGA (b) shows an expected load dependence. Peak values in the area of the full load curve are not discernible. This is due to the function of the EGA, which leads to homogenization of the exhaust gas temperatures. For the exhaust gas mass flow in (c), the load dependence is clearly visible. For the long-haul route, maximum exhaust gas backpressures (d) of up to 150 mbar, when measured at the outlet of the turbocharger, are to be expected for the downstream exhaust system.

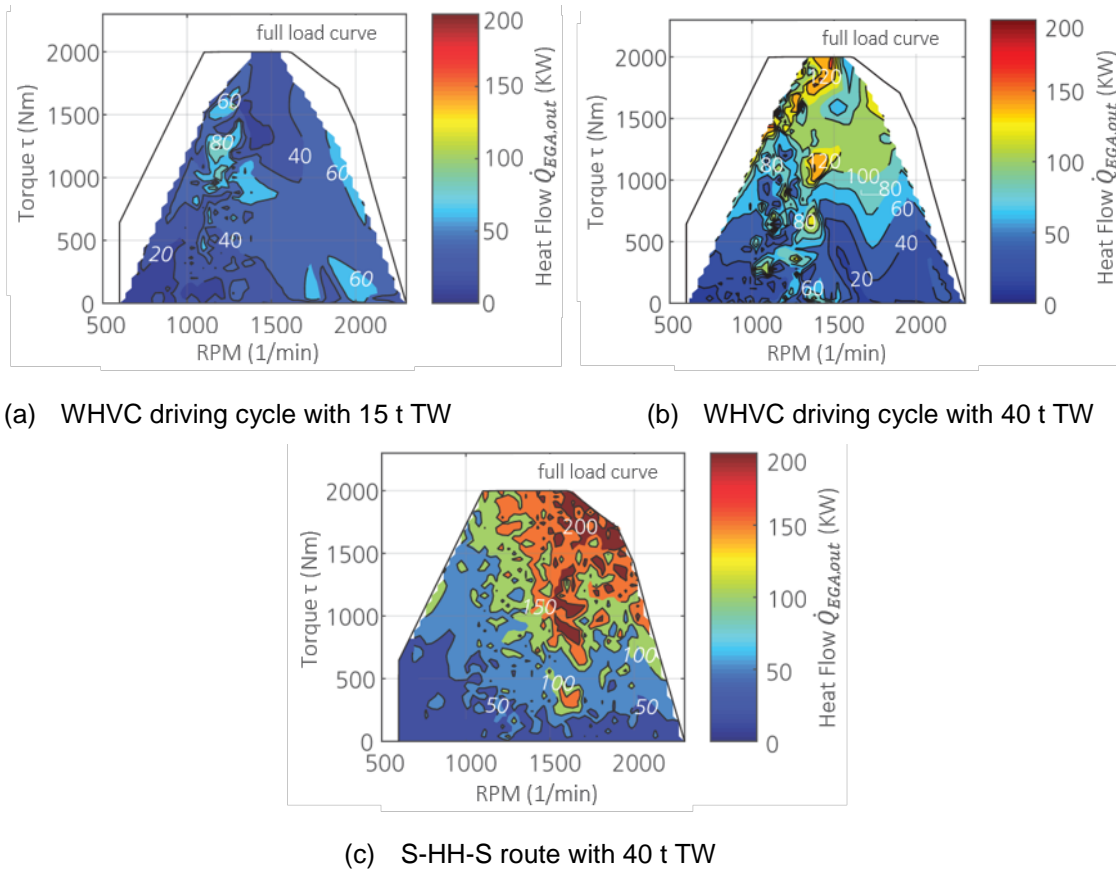


Figure 2-3 Potential analysis based on the available heat flows $\dot{Q}_{Ex,EGA}$ at the exhaust gas aftertreatment (EGA) outlet in the engine map.
(output data of the interpolation are based on dynamic simulation values)

Fuel consumption is load-dependent, i.e. depends on the required drive power. For higher load requirements, such as maximum vehicle load, demanding off-road profile, or high speeds, more fuel energy is needed, which, depending on the overall vehicle efficiency, leads to higher exhaust gas enthalpies and consequently higher usable heat flows. Examples of the heat flows are shown in Figure 2-3 for the WHVC driving cycle with 15 t TW (a) and 40 t TW (b) respectively, and for the real SHHS driving cycle with 40 t TW (c). The above-mentioned increase in the required drive powers and thus also in the available heat flows can be seen on the basis of these driving scenarios.

Table 2-6 serves as a summary of the results of the potential analysis. The index designation is used to identify the average (m) and maximum (max) operating points as well as the loading condition for the respective driving cycle or distance. Based on the

high exhaust gas temperatures $\vartheta_{EGA,out}$ compared to diesel heavy-duty vehicles (with more than 500 °C as an average value), high-temperature-stable TEMs such as skutterudite must be used for efficient TEG use. For more detailed results, see the Appendix for WHVC under Figure 5-1 and Figure 5-2.

Table 2-6 Overview of the defined operating points (OP) for the TEG design

OP	Designation	Ex. gas temp. $\vartheta_{EGA,out}$ (°C)	Ex. gas mass fl. \dot{m}_{EX} (kg/h)	Exhaust gas heat flow* $\dot{Q}_{EGA,out}$ (kW)	Exhaust gas exergy flow* $\dot{E}_{EGA,out}$ (kW)	Coolant temp. $\vartheta_{LT\ CC,in}^{*2}$ (°C)	Coolant vol. flow $\dot{v}_{LT\ CC}^{*2}$ (dm ³ /s)
1.1	WHVC _{15 t,m}	609	207	33.1	21.9	50	0.3
1.2	WHVC _{15 t,max}	659	564	96.2	64.8	43	0.4
2.1	WHVC _{40 t,m}	652	351	63.6	43.9	52	0.3
2.2	WHVC _{40 t,max}	710	776	169.4	118.0	46	0.4
3.1	SHHS _{40 t,m}	676	490	94.5	65.2	54	0.4
3.2	SHHS _{40 t,max}	743	1284	275.3	195.8	58	0.6

* in relation to ambient temperature $\vartheta_U = 20$ °C

*2 Data for the considered low temperature coolant circuit (LT CC)

In addition to the thermodynamic conditions, the geometric boundary conditions for the integration concept should also be taken into account. The outer visible area of the exhaust system of the tractor unit is shown in Figure 2-4. The reference vehicle is equipped with a three-way catalytic converter. As mentioned, the TEG should be positioned at the outlet of the EGA. Two positions were considered. Firstly, directly behind the EGA (i.e. between the EGA and the rear silencer) and, secondly, behind the rear silencer. In both cases, this could probably be made smaller as the TEG takes over part of the function. The positioning is thus primarily dependent on the required size of the TEG, which can be seen from the result of the overall systemic TEG simulation. If the TEG is so large that it can only be integrated after the rear muffler, it is highly likely that the tank volume will have to be reduced unilaterally. The analysis of the installation space investigation has shown that, in the first-mentioned position (between the longitudinal beams), a volume of max: 550 x 360 x 360 mm³ or, in the second position (outside the longitudinal beam), a maximum volume of: 750 x 800 x 600 mm³ is available.

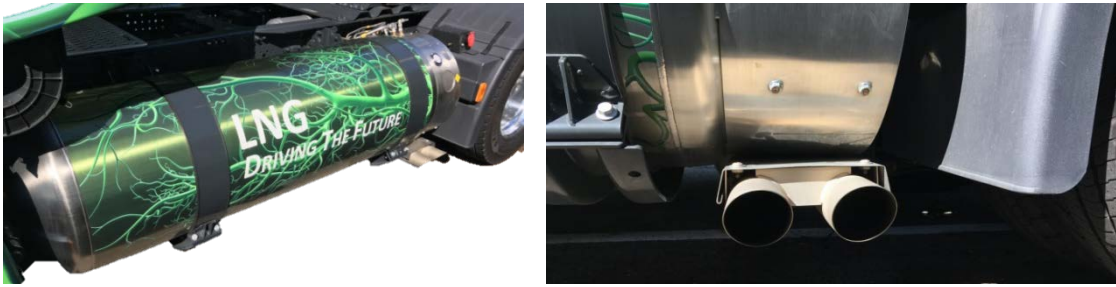


Figure 2-4 Detailed images of the vehicle and installation space assessment in the area of the exhaust system of the IVECO Stralis NP460 LNG

2.3 WP 3: Simulative overall system interactions

This section describes work contents in brief. For more detailed results, please refer to the Appendix in chapter 5.

2.3.1 Engine and exhaust gas aftertreatment

The aim of the work package is to build a flow model for a selected gas engine, then to map an exhaust gas aftertreatment system according to the engine's operating concept and to represent the entire gas path system virtually. This means that modeling and tuning are carried out without concrete measurement data on the engine and component test bench, but using the empirical values and prior knowledge of engine technology available at the FKFS Institute.

Design of the air and fuel path

The basic design of the air and fuel path of the combustion engine is taken from a heavy-duty vehicle diesel engine with model designation D2676 from MAN. The modeling of the engine flow model is carried out by fitting the air and fuel path from the previously mentioned model. The second step of the modeling includes the tuning of the combustion process of the engine. To describe the combustion process of the engine, the combustion model based on phenomenological approaches is developed using the "FkfsUserCylinder"® plug-in module. Finally, the turbocharger is adapted to the engine model. A model of the turbocharger is set up using the scaling methods already available at the FKFS Institute. The modeling of the engine is carried out entirely in the software environment of GT-Power from Gamma Technologies (GT).

Within the scope of this project, a 6-cylinder heavy-duty vehicle gas engine in a series arrangement with model designation Cursor-13 from FPT Motorenforschung AG (before 2012, Iveco Motorenforschung) is selected as the test vehicle (see Table 5-1 and Figure 5-3 in the Appendix). The engine has intake manifold injection and is spark ignited. A single-stage exhaust gas turbocharger with a controlled exhaust gas bypass valve (wastegate) is used to turbocharge the engine. The engine is operated stoichiometrically ($\lambda = 1$) and without exhaust gas recirculation (EGR). A three-way catalytic converter is installed downstream of the engine and enables simultaneous reduction of all pollutant emissions. In summary, the following steps were taken to implement the modeling:

- Adaptation of the air and fuel path
- Tuning of the combustion process
- Modeling of the exhaust gas turbocharger with a scaling method

Modeling of the exhaust gas aftertreatment system

Since the Cursor 13 gas engine available for the study is operated with $\lambda = 1$, a three-way catalytic converter is sufficient for exhaust gas purification. This consists of a metallic housing in which a ceramic or metallic carrier is supported on swelling or fiber mats to prevent breakage. The carrier – also known as substrate – must meet very high requirements in terms of mechanical and thermal strength. It has a mainly round, oval or rectangular shape in cross section. The beam is traversed in the axial direction by a large number of small, thin-walled so-called ‘honeycomb’ channels that are either round, triangular, rectangular or hexagonal in shape.

The three-way catalyst is modeled using a 1D surface reaction method. A variety of models exist in the literature describing the complex reaction diagram of a three-way catalyst. [5] provides an overview of the different reaction models. This report takes the model from the tutorial of GT-Power, which refers to a publication from Holder [6], as the basic model. When tuning the model, the reaction mechanisms in the basic model (that was originally used for gasoline operation) are adjusted accordingly to the requirements for the application of the catalyst for gas engines.

The information on the geometry, materials and structure of the catalyst needed for the modeling comes from the empirical data available at the FKFS. The three-way catalyst model is connected with the air and fuel path model via an interface. The interface allows the use of different numerical solvers in one model to speed up the calculation with chemical reactions. The pressure losses in the catalytic converter are matched to those in the particulate filter from a diesel heavy-duty vehicle using the multiplier for pressure losses.

Simulation results in engine maps

Figure 2-5 shows the simulation results of the model for the internal combustion engine for fuel consumption and raw emissions. Although the model was created from empirical values and estimated data only, it basically outputs results with plausible orders of magnitude and can describe the engine behavior qualitatively.

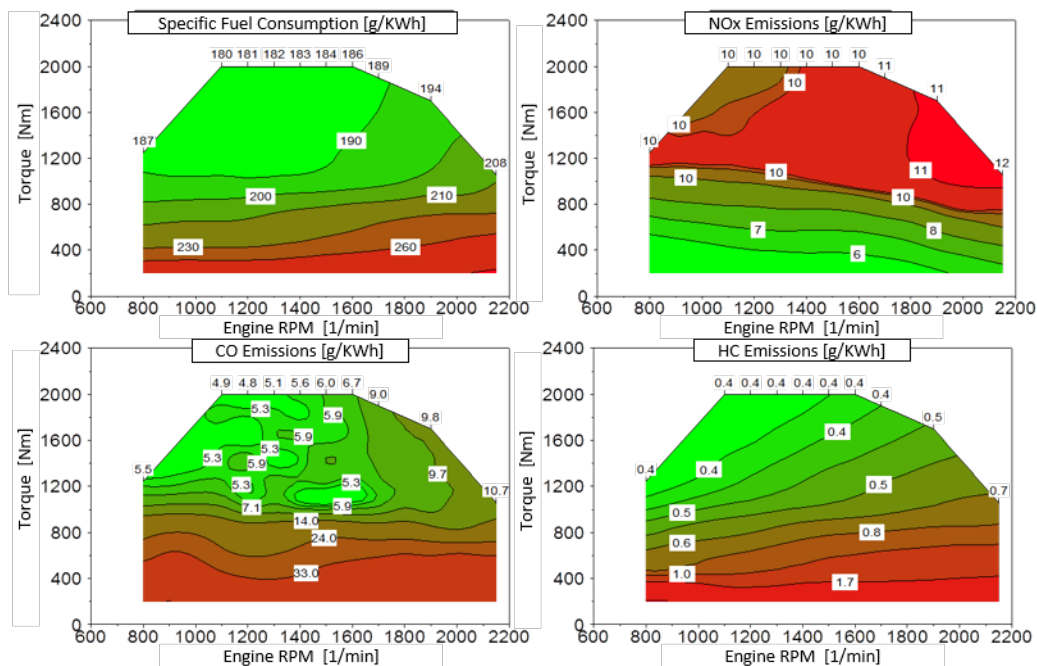


Figure 2-5 Simulation results for fuel consumption and raw emissions as a function of engine speed and engine torque

Further results of exhaust gas temperatures and mass flows, I_K value (knock limit) and pressure losses in the three-way catalyst, as a function of engine speed and torque are shown in the Appendix in Figure 5-4.

Simulative study for emissions and influence of pressure losses on fuel consumption

Since 2013, the World Harmonized Stationary Cycle/World Harmonized Transient Cycle (WHSC/WHTC) have been applied as statutory test cycles for testing the HCV exhaust emissions. WHSC operating points determined in accordance with statutory procedures can be found in the Appendix in Figure 5-5 and Table 5-2. A simulation with the transient calculations of the thermal behavior, i.e. the temporal change of the exhaust gas temperatures in the three-way catalyst was carried out. It was shown that the three-way catalyst model works well and that the engine with the downstream exhaust gas aftertreatment system can meet the legal requirements for emissions. For details, please refer to Figure 5-6 in the Appendix. The legal limit values for exhaust emissions are indicated in black letters in the illustration. The values in red letters represent the simulation results and are calculated using the guidelines for calculating exhaust gas emissions in the WHSC.

The TEG is to use the exhaust gas temperature after the exhaust gas aftertreatment system. In doing so, the functioning of the catalytic converter should not be impaired. The exhaust gas temperatures occurring in the exhaust gas section at the WHVC operating points can be found in the Appendix in Figure 5-7. It can be seen that the exhaust gas temperatures at the outlet of the catalyst are higher than those before the catalyst at some operating points. This is due to the exothermic reactions in the catalyst. In the simulation, an exhaust pipe with a length of 60 cm made of carbon steel was used after the catalytic converter. The blue bars in the diagram represent the exhaust gas temperature at the end of this exhaust gas pipe. The integration of the TEG after the catalyst is advantageous because the influence on the EGA is considered to be comparatively low and the available temperatures can be higher depending on the load or operating point.

The TEG system in the EGA causes an additional exhaust gas backpressure due to the heat exchanger structure used. To push the exhaust gas out of the engine cylinder against the increased exhaust backpressure, more fuel must be injected into the cylinder and extra power must be applied to overcome the charge exchange losses. Initially, this will lead to rising fuel consumption. In order to qualitatively illustrate the influence of the increased exhaust backpressure on fuel consumption, simulations are performed with

the additional exhaust backpressures given to the engine model at the WHSC operating points. Due to the heat extraction of the exhaust gas when using the TEG, the density of the gas increases. This causes the flow velocity of the exhaust gas to slow down so that the pressure drop in the downstream components of the exhaust system decreases compared to the same operating point without heat extraction. Therefore, additional exhaust gas backpressures are given to the model with positive (up to 300 mbar) as well as negative values (up to -100 mbar). The detailed simulation results can be found in the Appendix in Figure 5-8 and Figure 5-9. It can be seen that the specific fuel consumption tends to increase linearly with increasing exhaust gas backpressure. The minimal fluctuations in the curves are due to slight changes in the lambda value in the exhaust gas. However, the lambda control in the model basically works well. The slight variations in the lambda value may be caused by the numerical solvers used simultaneously in the model.

2.3.2 Engine cooling

The TEG is cooled with the cooling medium from the engine cooling system and is essential for the function of the TEG. The objective of this sub-work package is to present the possible integrations of the TEG in the engine cooling system and the cooling system potentials for TEG application using 1D simulation.

Cooling system design

No measurement data or information regarding the cooling and oil circuit of the Cursor 13 gas engine is available as part of the project. Furthermore, the aim of the investigations is to qualitatively present the cooling potentials of a general heavy-duty vehicle cooling system for TEG application. It was therefore decided to derive the cooling system of the Cursor 13 gas engine from the existing cooling system of the MAN diesel engine. Some changes have to be made in the cooling system configuration taking into account the engine concept of the Cursor 13 gas engine. First, the Cursor 13 gas engine is supercharged with the single-stage exhaust gas turbocharger with the controlled bypass valve. Compared with the MAN diesel engine with two-stage turbocharging, only one intercooler is required. In addition, the EGR cooler used in the MAN diesel engine is no longer required, as the Cursor 13 gas engine is operated without EGR. The design of

the cooling system for the engine is shown in Figure 2-6 and the interconnection positions developed within the framework of the project are presented.

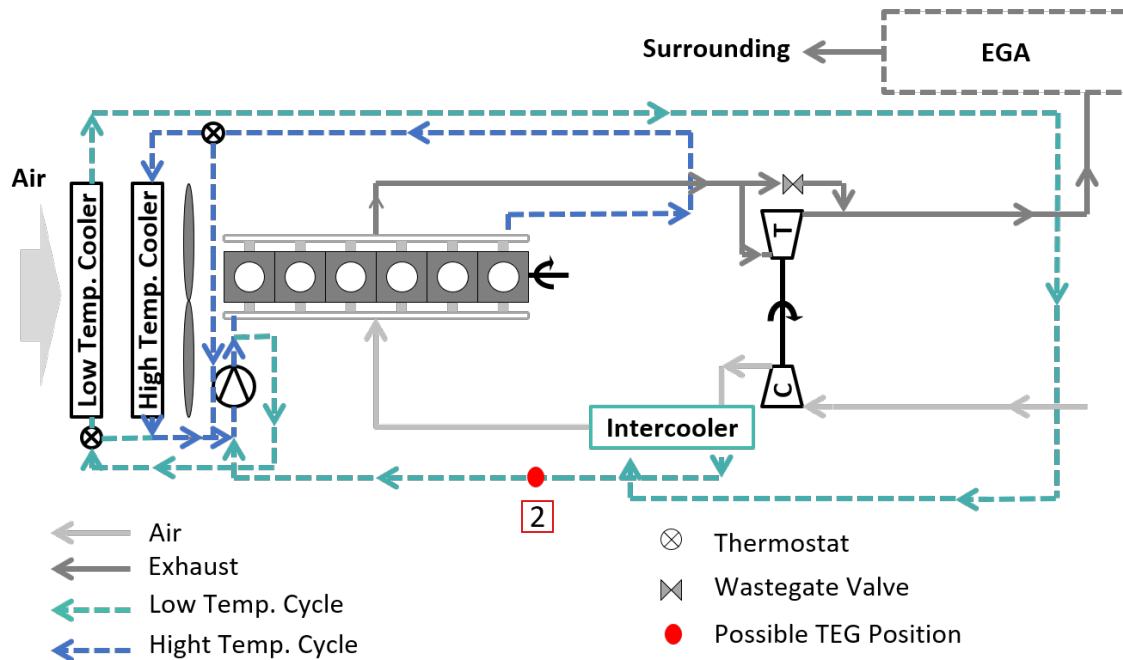


Figure 2-6 Design of the adapted cooling system for Cursor 13 gas engine

The cooling system has a high-temperature circuit (HT circuit) with a high-temperature cooler used to cool the combustion engine and a low-temperature circuit (LT circuit) with a low-temperature cooler used to cool the compressed fresh air. Two thermostats, a cooling medium pump and a fan are used as components for thermal management in the cooling system. The thermostats control the coolant mass flows through the high-temperature and low-temperature cooler to maintain the set coolant temperatures. During the warm-up phase, the thermostat in the high-temperature circuit is closed to warm up the combustion engine as quickly as possible. The coolant pump is mechanically operated by the motor and has a fixed transmission ratio between pump and motor speeds. The task of the vehicle fan is to increase the air mass flows through the radiator when the radiator cooling capacity is insufficient, e.g. when the vehicle is traveling at low speeds or driving uphill with a maximum load. The fan is operated by the motor via a viscous coupling with varying transmission ratios. The function of the entire thermal management system is to ensure the optimum thermal conditions of the combustion engine at the varying driving speeds and ambient temperatures.

Cursor 13 gas engine cooling system model

The cooling system adapted for the Cursor 13 gas engine is modeled in GT-Suite using a 1D method (finite volume method). The cooling system has 18 l of ethylene-glycol-water vol. 50/50 mixed refrigerant. The high-temperature cooler can dissipate 240 kW of heat at the design point, which is at the rated speed of the MAN diesel engine, with a minimum required coolant circulation rate of 390 l/min. The low temperature cooler can dissipate 106 kW of heat at the same operating point with a minimum required coolant circulation rate of 45 l/min. The models of the two coolers are used unchanged for the cooling system of the Cursor 13 gas engine. To adapt the existing cooling system to the Cursor 13 gas engine, the engine structure in particular is modified in a similar way to the air and fuel path model. Then, the calculation results of the heat balance (presented in Figure 2-7) are used with the cooling system model. These calculation results are used to characterize the thermal interaction of the combustion chamber with the surrounding walls and are stored as maps in the cooling system model.

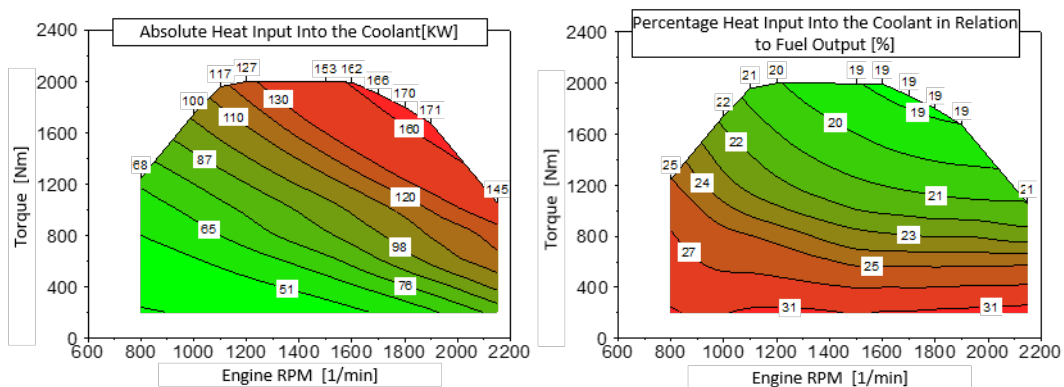


Figure 2-7 Heat balance map as a function of engine speed and torque from simulation results with the air and fuel path model. Left: Absolute heat input into the coolant in kW; Right: Percentage heat input into the coolant in relation to fuel output in %

The cooling potentials at the varying operating points can be numerically investigated using the adapted model of the cooling system from the Cursor 13 gas engine. A prerequisite for the investigations is that the heat dissipation from the TEG into the cooling system should not cause any additional performance of the vehicle fan. A simulation for the cooling system with basic design was therefore first performed to

calculate the transmission ratio between engine and fan speeds. The results of these simulations are shown in the Appendix in Figure 5-11 for three different driving speeds.

Investigation of the cooling potentials of the cooling system with regard to TEG application

Since the engine cooling system is designed for extreme driving conditions such as hill driving at lower driving speeds with maximum payload, there is potential for additional heat dissipation in most driving situations. These cooling potentials at the various operating points can be exploited for TEG applications. In order to illustrate the potentials of heat dissipation from the TEG into the cooling system and the resulting influences on thermal state changes of the engine cooling system, different integration concepts are investigated in this section using the adapted model of the cooling system presented in the previous section.

The engine cooling system has three circuits: Short circuit, high temperature circuit and low temperature circuit. The short circuit is used in combination with the thermostat in the high temperature circuit both to warm up the engine and to adjust the temperature of the engine structure during warm operation. The short circuit is integrated into the motor structure and is not suitable for TEG application. Nevertheless, high-temperature and low-temperature circuits are available for integrating the TEG in the engine cooling system. After detailed investigations that are included in Interim Report I, two possible integration positions of the TEG in the cooling system are determined, which are marked in Figure 2-6 with the red dot markings. The heat dissipation $\dot{Q}_{Zu_Potential}$ from the TEG into the cooling circuit can be calculated in principle according to equation (4) of the Appendix.

Investigation of the cooling potentials by means of simulation

The fan ratios are specified in the following calculations of the cooling potential. The cooling potential of the cooling system with integration of the TEG are then calculated for interconnection option 1, i.e. interconnection of the TEG after the HT cooler (see Figure 2-6). Here, the coolant temperature at the engine outlet of 91 °C is used as the target value, i.e. heat is supplied to the cooling system until the coolant temperature at the engine outlet reaches 91 °C. In addition, another restriction is given in the simulation

that the coolant temperature of the pipe sections must not exceed 100 °C immediately after the heat is applied. The results of the simulations are shown in Figure 2-8.

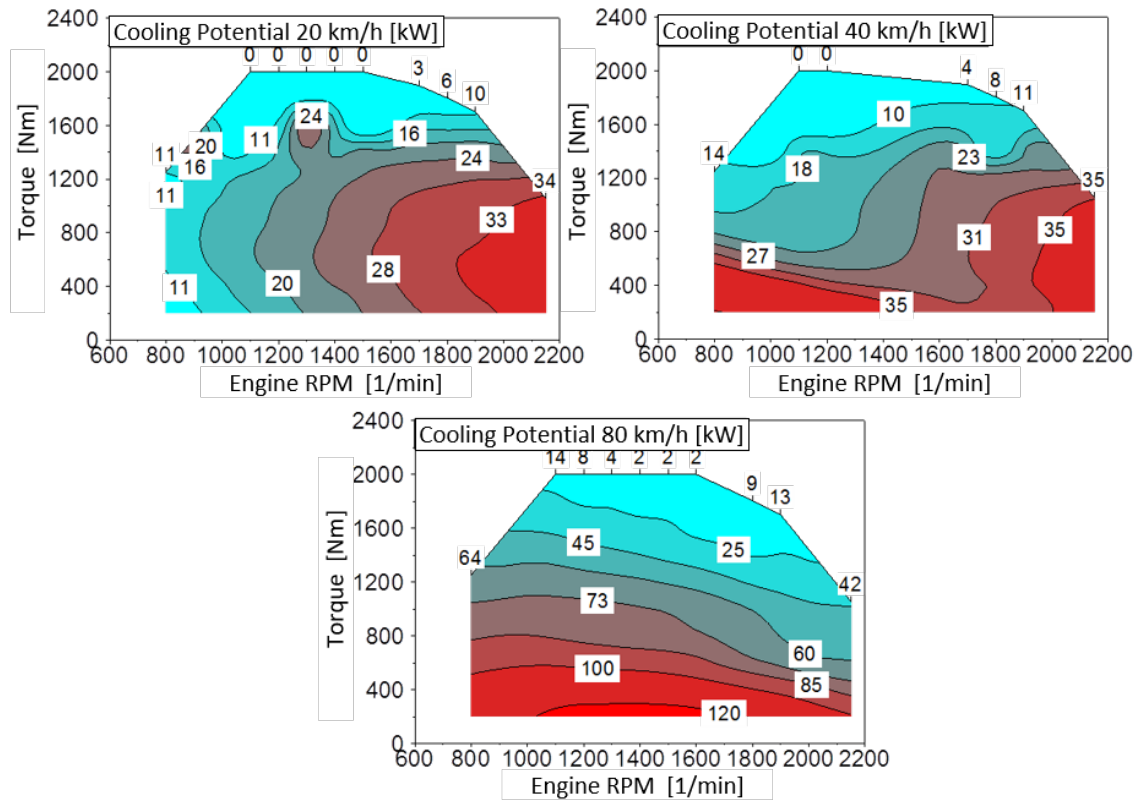


Figure 2-8 Simulation results for cooling potentials of the cooling system when the TEG is connected after the HT cooler with coolant temperature at the engine outlet of 91 °C as the target value at the different driving speeds under ambient temperature of 20 °C

The simulation results of the cooling potential of the cooling system for the same integration position of the TEG, but with the coolant temperature at the engine outlet of 100 °C as the target value, can be found in the Appendix in Figure 5-11. Figure 5-12 shows the results of the calculation of the cooling system's cooling potentials when the TEG is connected after the intercooler in the LT circuit, integration position 2 (see Figure 2-6).

The cooling system's cooling potentials at low driving speeds tend to be dependent on the engine speeds due to the operation of the fan. As driving speeds increase, cooling potentials become more dependent on the engine loads.

Another simulation for constant runs on the level of the 40-tonne heavy-duty vehicle with Cursor 13 gas engine for the 12th gear was carried out on the basis of the known information about the vehicle and the empirical values for HDVs available at the FKFS (see Table 5-3 in the Appendix). Figure 2-9 shows an example of the maximum permissible heat dissipation of the TEG into the cooling system for the circuit variants explained above.

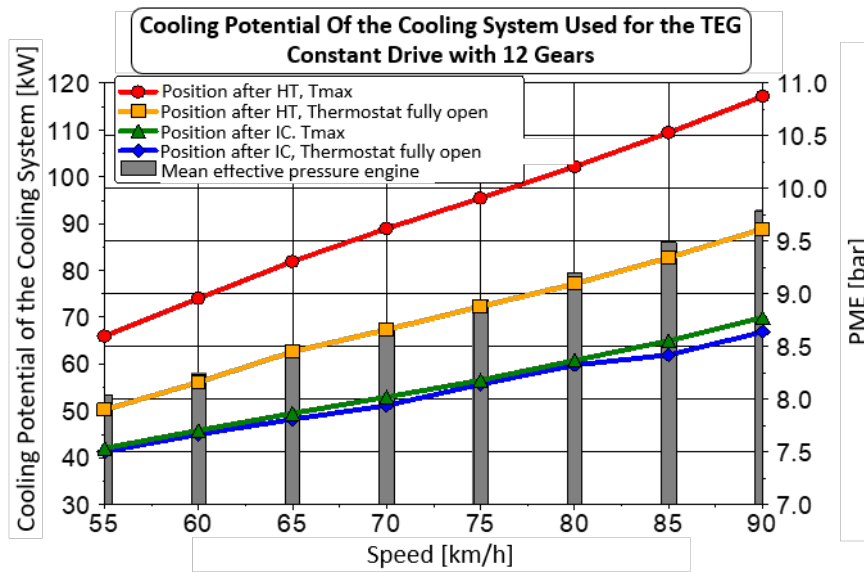


Figure 2-9 Maximum permissible heat dissipation of the TEG into the cooling system during constant driving on the level in the HDV with Cursor 13 gas engine for different integration positions of the TEG (12th gear, vehicle mass with 40 t payload, ambient temperature 20 °C)

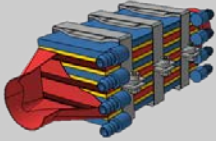
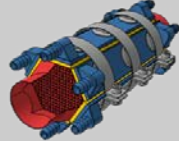
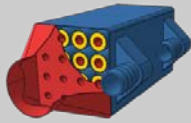
2.4 WP 4: Constructive TEG design

2.4.1 Methodical concept and solution finding

To design a TEG in the new application area, the design concept must first be determined. Table 2-7 shows the possible design variations. A preliminary study was required due to the low level of prior experience in heavy-duty vehicle applications and the large differences in the approach of the state of the art, as shown in chapter 2.1.

As a result of this, the tube bundle design appeared unsuitable for HDV applications due to its low efficiency, problems with thermomechanics, and high system costs. The stacked design method offers advantages based on the evaluation criterion of the cost-benefit ratio compared to the polygonal construction method. The latter design may provide greater benefits based on the gross and net performance under specific boundary conditions, but this is negated by the significantly higher costs. For this reason, further development was based on the architecture design.

Table 2-7 Overview of conventional TEG configurations, figures from [7]

	Stack Architecture	Polygon Architecture (e.g. hexagon)	Tube Bundle Architecture
Examples ¹ :			
Research Application:	car, truck	car, truck	car, truck
HEX-Form:	flat-plate fins	honeycomb or swirl fins	pipe cluster
TEM-Form:	flat-plate	flat-plate	round center hole

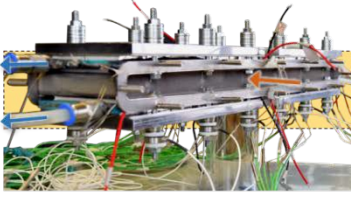
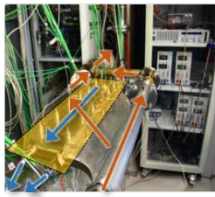
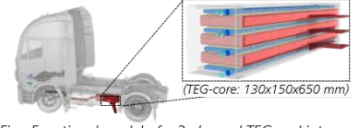
The system components, such as the heat exchangers (HEX) must be dimensioned for TEG use in the HCV application. As a feasibility study and as a test of the function of the construction method in the HCV dimension and for validation of the TEG simulations, a functional sample is required as part of a preliminary or validation study.

2.4.2 Validation study

For this study, a partial setup of the TEG system as a single-channel TEG, i.e., one hot gas heat exchanger (HGHEX) and correspondingly two coolant heat exchangers

(COHEX), was designed based on the holistic simulation. Commercially available thermoelectric modules (TEM) of the SnSe material class were used. The results of the validation study as well as the resulting cost-benefit optimum of the 3-channel TEG setup integrated into the reference vehicle is shown in Table 2-8. The TEG design would deliver an electrical output of up to 1510 W under optimum conditions in OP_{max} at a unit cost (high number of units typical of HDV) of 1811 EUROS. Even under the theoretical assumption that this TEG system would be operated permanently in OP_{max} , the system would reduce fuel consumption by only 0.5 % and would only be amortized after a significantly longer period than 3 years in the deployment scenario defined (see chapter 2.5.2). This result shows that the commercially available modules and their design of the state of the art are not suitable to meet the project objectives and present a sufficiently low cost-benefit ratio for HDV use. Instead, during the course of the project, a TEM developed specifically for the HDV application was developed and considered in collaboration with a module manufacturer.

Table 2-8 Results of the preliminary investigation with commercial TEMs based on the preliminary study

Name	Fs.	Simulation	Experiment	Figure
TEM-Material	-	SnTe _{1-x} Se _x	SnTe _{1-x} Se _x	  <p>Fig.: Functional model of a single channel TEG</p> <p>Fig.: Experiment of a single channel TEG</p>
TEM-Number	n_{TEM}	56	56	
Electrical Power ¹	P_{El}	405 W	282,9 W*	
Back Pressure ¹	Δp_{TEG}	22 mbar	25,9 mbar	
Efficiency ¹	η_{max}	3,7 %	2,5 %*	
	η_M	3,4 %	3 %*	
Weight**	m_{TEG}	6 kg	6,8 kg	
TEM-Number	n_{TEM}	168	-	 <p>Fig.: Functional model of a 3-channel TEG and integration into a LNG heavy duty vehicle</p>
Max. Elect. Power ²	$P_{El max}$	1.510 W	-	
Back Pressure ²	Δp_{TEG}	32 mbar	-	
Weight**	m_{TEG}	30,2 kg	-	



¹ Boundary condition BP: $\vartheta_{Ex}=550\text{ }^\circ\text{C}$, $\dot{m}_{Ex}=300\text{ kg/h}$, $\vartheta_{Cc}=85\text{ }^\circ\text{C}$, $\dot{m}_{Cc}=5\text{ l/min}$.

² Boundary condition BPmax: $\vartheta_{Ex}=550\text{ }^\circ\text{C}$, $\dot{m}_{Ex}=900\text{ kg/h}$, $\vartheta_{Cc}=5\text{ }^\circ\text{C}$, $\dot{m}_{Cc}=20\text{ l/min}$.

* Deviation due to lower contact pressure and due to manufacturing tolerances.

** Specification for the TEG core without measurement technology.

Explanation:

-  Hot gas mass flow
-  Coolant mass flow

2.4.3 Dimensioning

The dimensioning of the TEG core, consisting of the heat exchangers with the TEMs and the bracing device, is largely determined by the number and arrangement of the thermoelectric modules. In the stacked design concept, a large number of stacks of alternating HEX and TEM are positioned on top of each other, and the position is fixed by a pretensioning device. Simulation results indicate an optimal cost-benefit ratio of the system with three TEM strips in the flow direction (x-coordinate) (see Figure 2-24). As a result, 144 TEMs with dimensions about $31 \times 31 \times 3.4\text{ mm}^3$ (see selection chapter 2.5) are to be used and the distance between the modules is to be 1 mm each. This results in a total active area of about $95 \times 152\text{ mm}^2$ (module area of about 0.14 m^2).

Table 2-9 Dimensioning the number of TEG stacks

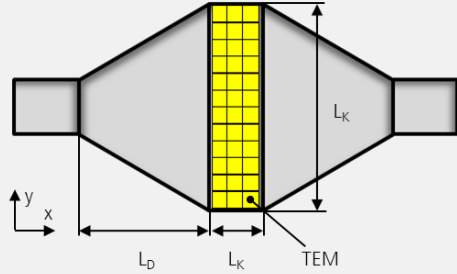
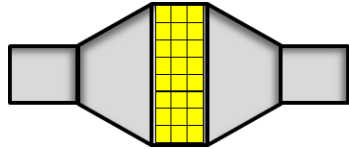
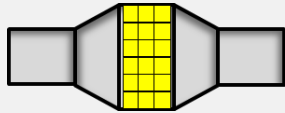
Stack (-)	L_k (mm)	B_k (mm)	L_D (mm)	Top view (sectional view at module level)
2	94	381	243	
3	94	254	133	
4	94	191	79	

Table 2-9 shows a listing of the TEG geometries with the relevant stacking numbers 2, 3 and 4 in the TEG core and the diffuser and confuser. The exhaust gas pipe is shown as a 4" pipe with a diameter of around 100 mm. According to [8], the opening angle of a diffuser and confuser of an exhaust gas system should not exceed 30°. Otherwise, flow separations occur, which causes an inhomogeneous flow distribution and generates an increased backpressure. The exhaust gas inlet and outlet pipes are dimensioned according to this boundary condition. It is possible to see the significant reduction in size – and thus the volume – of the TEG when the number of stacks is increased in the figure. A smaller size results in lower space requirements and thus also lower weight, as well as greater mechanical stability. At the same time, however, a higher number of stacks means higher costs in the manufacture and assembly of the TEG. The best results in the combination of the influencing criteria are achieved with 3 stacks, the size is significantly smaller than that of the variant with 2 stacks and the number of stacks is justifiable in terms of production costs.

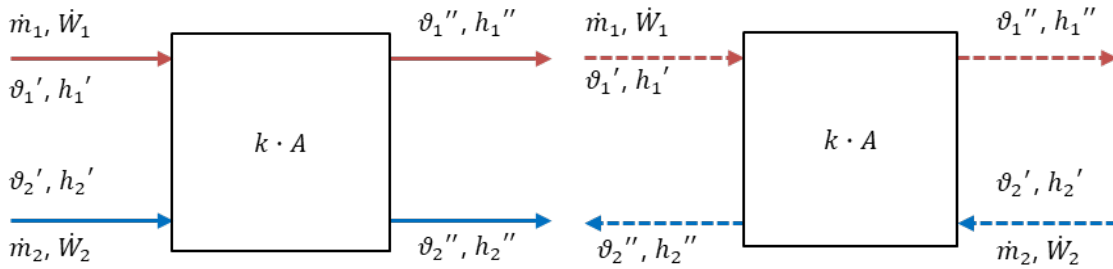
2.4.4 Results of the design process

Heat exchanger (HEX) concept

A TEG consists for the most part of arranged heat exchangers, as can be seen in Table 2-7 by means of the red and blue colored components. The design of these HEXs plays an important role for the conceptualization and interpretation of the TEG. In principle, the DLR's stacked design approach uses indirect heat transfer with plate heat exchangers of the two media. The flow routing of the hot exhaust gases of the combustion engine dominates the design, the routing of the second medium cooling water is subordinate. In general, for good efficiency of the heat exchanger, the components separating the media should have good thermal conductivity and large surface area. Turbulent flow is favorable for good heat transfer. This occurs mainly at high Reynolds numbers. The flow velocity should therefore be kept high and the viscosity of the media should be low. It should be noted that high velocities and large wetted surfaces also require a high energy input to "pump" the media through the heat exchanger. Two different media are used in the TEG's HEXs, one is liquid and one is gaseous. Therefore, the heat capacities per volume of the media differ greatly. Optimally, the gaseous fluid flow should be significantly greater than the liquid flow. The surface for heat transfer should be increased on the gas side. This can be done, for example, by ribbing.

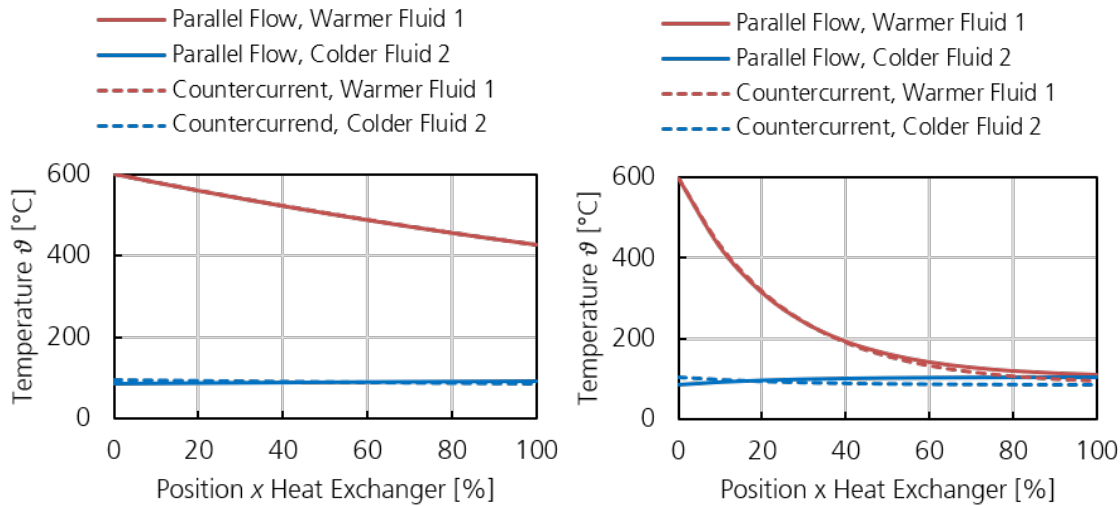
The heat transfer performance and the corresponding efficiency depend mainly on the heat transfer coefficient k and the transfer surface A (see Figure 2-10 (a) and (b)). The extent of heat transfer is also strongly dependent on the geometric guidance of the two material flows relative to each other, which is shown using an example below. The basic shapes that can be considered for stacking are the co-current, countercurrent with symmetrical structure and the cross current with asymmetrical structure in their pure form, or also with cross-mixing. In terms of thermal performance, countercurrent represents the most favorable current flow, while direct current represents the least favorable. Depending on the selected aspect ratio of length L to width B , the cross-flow structure lies between the two mentioned, and is therefore not shown. The difference in flow guidance is strongly dependent on the size of the selected transfer surface A_{HEX} , as shown in Figure 2-10 (c) and (d). In addition, the distinction refers only to the thermal

and not to the thermoelectric design, where other criteria such as electrical power, cost, and weight are decisive, which can lead to a different choice of flow routing.



(a) Parallel flow HEX

(b) Countercurrent HEX



(c) $A_{HEX} = 0,1 \text{ m}^2$

(d) $A_{HEX} = 1 \text{ m}^2$

Figure 2-10 Schematic representation of a pure co-current (a) or pure countercurrent heat exchanger (b) as well as fluid flows along the heat exchangers with different heat exchanger surfaces A ((c), (d), boundary conditions: $\vartheta_1' = 600 \text{ }^\circ\text{C}$, $\dot{m}_1 = 350 \frac{\text{kg}}{\text{h}}$, $\vartheta_2' = 85 \text{ }^\circ\text{C}$, $\dot{m}_2 = 10 \text{ l/min}$)

For heat exchanger surfaces ($A_{HEX} < 0.5 \text{ m}^2$) flow routing plays a subordinate role, since, for the considered system specifications, the difference of the transferred thermal power is $\Delta \dot{Q}_h < 2 \%$ and the difference of the mean log temperature difference is $\Delta T_m < 2 \text{ K}$. The objective of this project is to develop a TEG with high efficiency. For this reason, a countercurrent HEX is selected for the system design.

Functional model

Figure 2-11 shows the functional model of the TEG result design as 3-channel TEG. The housing shape is shown in (a). The flange is designed with a V-band clamp. The housing is designed around the TEG core and diffuser to accommodate the axial thermal expansions due to the metal bellows in a round design – as described in section 2.4.3. The mechanical rigidity of the housing is also increased by beading to counteract possible vibrations. The functional model also has maintenance flaps on both sides to allow changes to the measurement technology or further hardware configurations to be carried out. The same representation is illustrated with transparent housing in (b).

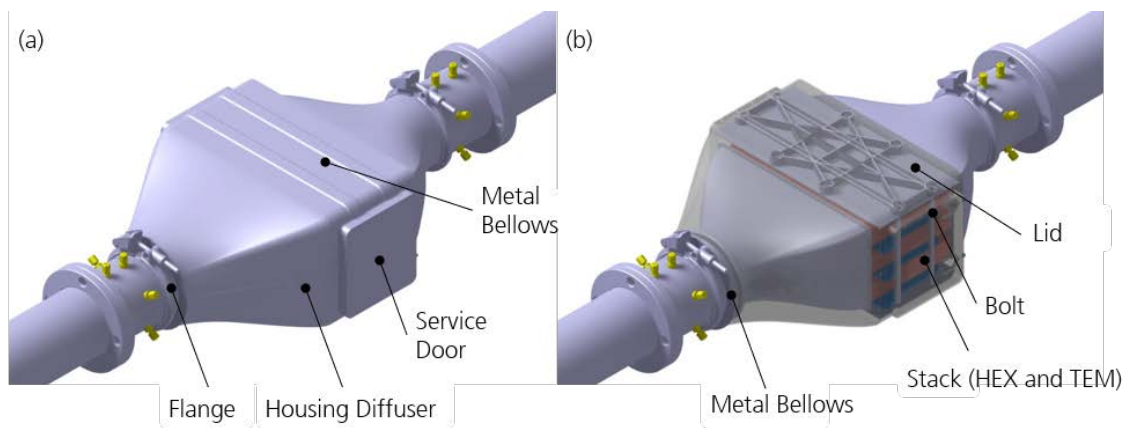


Figure 2-11 CAD model of the 3-channel TEG result design as a functional model for experimental validation (a) and with transparent housing components (b)

The metal bellows can be seen directly behind the flange and in front of the diffuser. In the TEG core, the three hot gas heat exchangers are designed as a stack, and the total of eight bolts and the cover apply the necessary surface pressure with the appropriate bolt tensile force. The lid has ribs between the bolts and above the TEM for additional stiffening. The increased rigidity means the contact pressure is distributed more evenly and thus efficiently to the TEM. The functional model has the dimensions (length/width/height) including maintenance flaps and diffuser/confuser: 530 x 355 x 180 [mm]. It therefore meets the requirements of the available installation space in the exhaust gas system of a natural gas HDV (see chapter 2.2).

Test rig

The functional model was tested experimentally on the DLR hot gas test rig that was converted to the new dimensions in the heavy-duty vehicle sector for this purpose. This primarily concerns the pipe diameter that has been expanded to 4" (see Figure 2-12). This reduces possible turbulence from the combustion chamber and other inhomogeneity, comparable to the installation position behind the EGA in the reference vehicle. A measuring ring is fitted upstream and downstream of the TEG functional model to record the exact inlet temperatures along the pipe radius and the pressure drop across the test specimen. In the outlet area, another section is installed to reduce external influences. This setup ensures a measurement with defined boundary conditions.

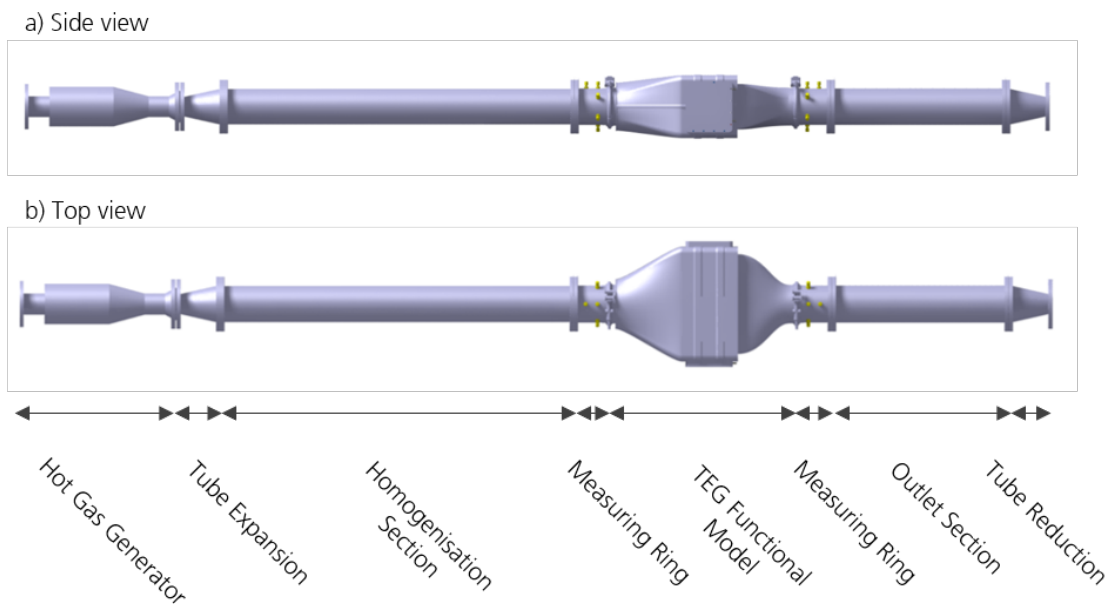


Figure 2-12 Design of the test rig structure

Vehicle integration concept

The potential and target vehicle integration of the TEG is shown in Figure 2-13. The exhaust gas system and the TEG are highlighted in red. For the first time, due to the increase in power density of the TEG system and the resulting low TEG volume, it was possible to fully integrate it in the EGA of the reference tractor unit for long-distance transport. This high level of integration directly downstream of the three-way catalytic converter is very advantageous. The exhaust gas enthalpies are higher due to the exothermic reaction of the catalyst depending on the load. The influence on the EGA is comparatively low, and the downstream rear silencer means that large flow cross sections are conceivable during implementation. This creates synergy effects. Similarly, with this integration, only one common housing can be used and the silencer can be smaller in size due to reduced flow velocities and damping in the TEG. A bypass flap at the end of the section appears to be sufficient and can be implemented in the design space. Such integration is considered to be purposeful for future development work.

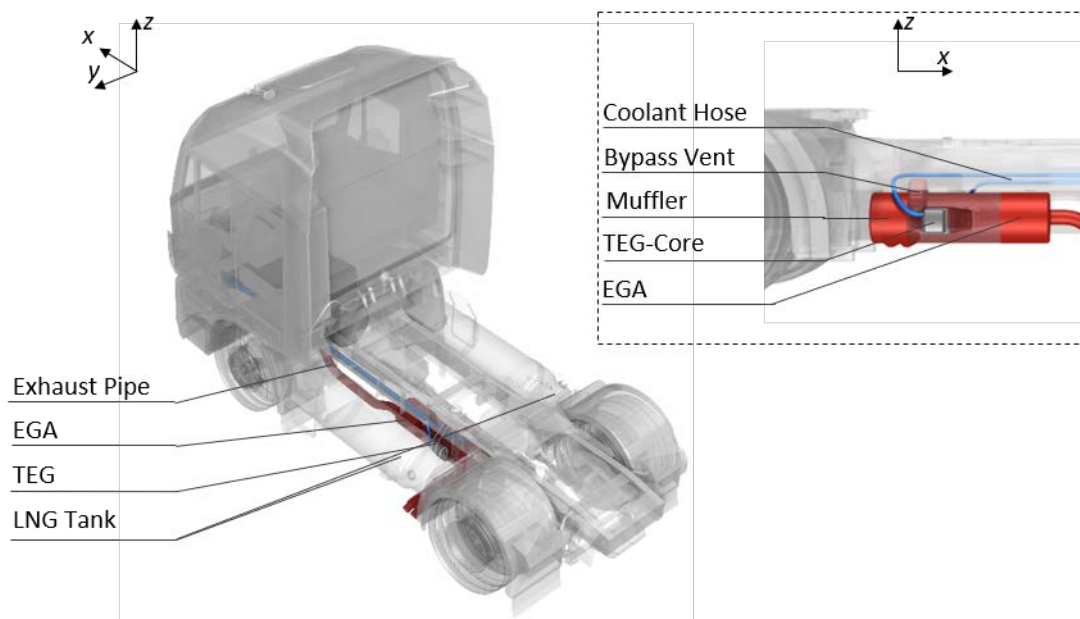


Figure 2-13 3D CAD model of the TEG installation concept in the exhaust system (colored red) of the reference vehicle of the natural gas tractor unit

2.5 WP 5: overall systemic TEG simulation

2.5.1 Vehicle interactions

The simulation of the TEG system follows a holistic approach, i.e. taking into account all vehicle interactions and the cost-benefit ratio. The target represents the first-time achievement of the intended amortization period of < 2 years. The existing vehicle interactions are shown in context in Figure 2-14.

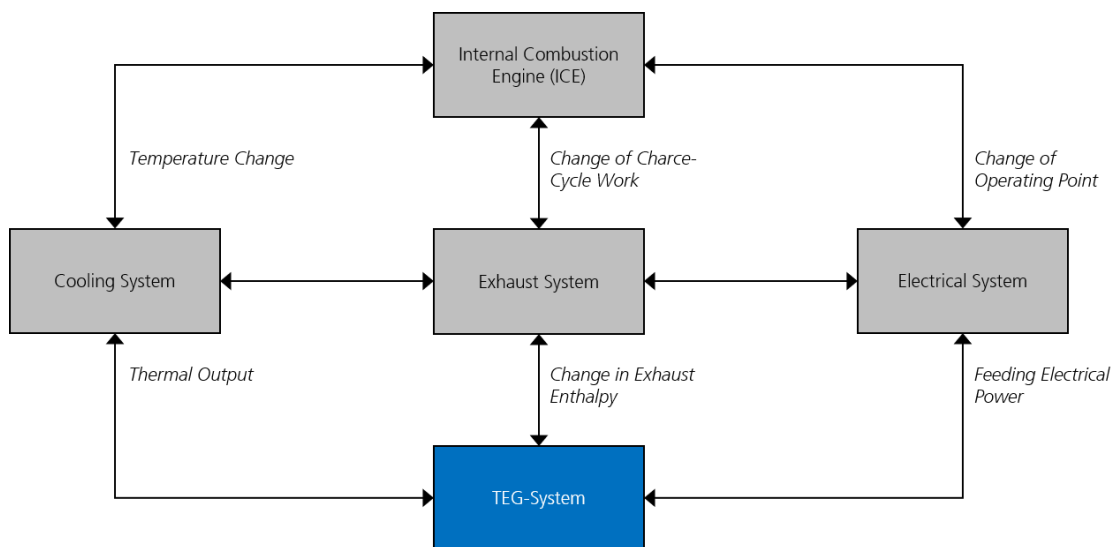


Figure 2-14 TEG as a subsystem in the overall vehicle system and its interactions

The simulative approach and the optimization strategy follow the defined project objectives and focus on the lowest possible cost-benefit ratio and a low amortization period of the TEG components (in typical constant driving, in semitransient driving scenarios and in specific driving cycles).

Vehicle interaction with the internal combustion engine

The influence of the TEG system on the internal combustion engine is primarily due to the change in the load change work due to the additional backpressure of the TEG, the change in the engine operating point, amended coupling of the alternator and the additional weight. The increased heat flow of the TEG into the vehicle cooling system can also influence the combustion engine based on the changed coolant temperature.

The aspects addressed are all considered according to the holistic approach. The load point displacement is represented by the Willans lines approach and a longitudinal dynamics simulation. The influence of the additional weight is also determined. For the consideration of the exhaust backpressure, a load point dependent correlation, based on the performed 0/1D simulations of the FKFS from WP 3 (for details, see chapters 2.3.1, Figure 5-8 and Figure 5-9 in the Appendix), as can be seen in Figure 2-15 using the three-dimensional polynomial interpolation, has been established.

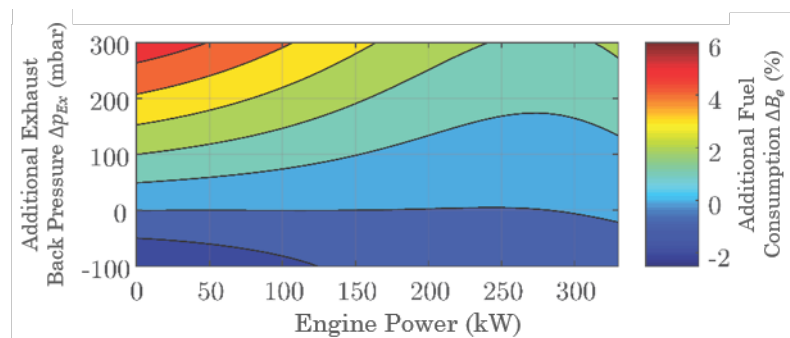


Figure 2-15 Resultant change in fuel consumption when the exhaust gas backpressure of the exhaust gas system of the reference vehicle is changed with varying engine output

Vehicle interaction with the cooling system

The basics of the reference vehicle and its cooling system were determined in chapter 2.3.2. Based on the results presented there, correlations were derived and incorporated in the overall systemic TEG simulation. Among other things, this takes into account the additional heat capacity of the cooling system until the vehicle fan is switched on.

Vehicle interaction with the on-board electrical system

Feeding the converted electrical power of the TEG from the exhaust enthalpy is the basis for reducing the fuel consumption. A conventional 24-volt on-board electrical system architecture (for state of the art, see Figure 2-16) was considered in the project. Primarily, the TEG replaces the vehicle's electrical generator that produces a rated current of 90 A to supply the electrical loads. The demand of the loads varies depending on the vehicle configuration and driving distance and is in the range of 600 to 1500 W for conventional HCV. Within the framework of the project, an average on-board electrical system requirement of 1025 W was taken as a basis according to [9] and [10]. Provided that the TEG system generates a greater power, the rechargeable batteries are charged with a nominal capacity of 220 Ah, up to the (maximum) state of charge of 90 %.

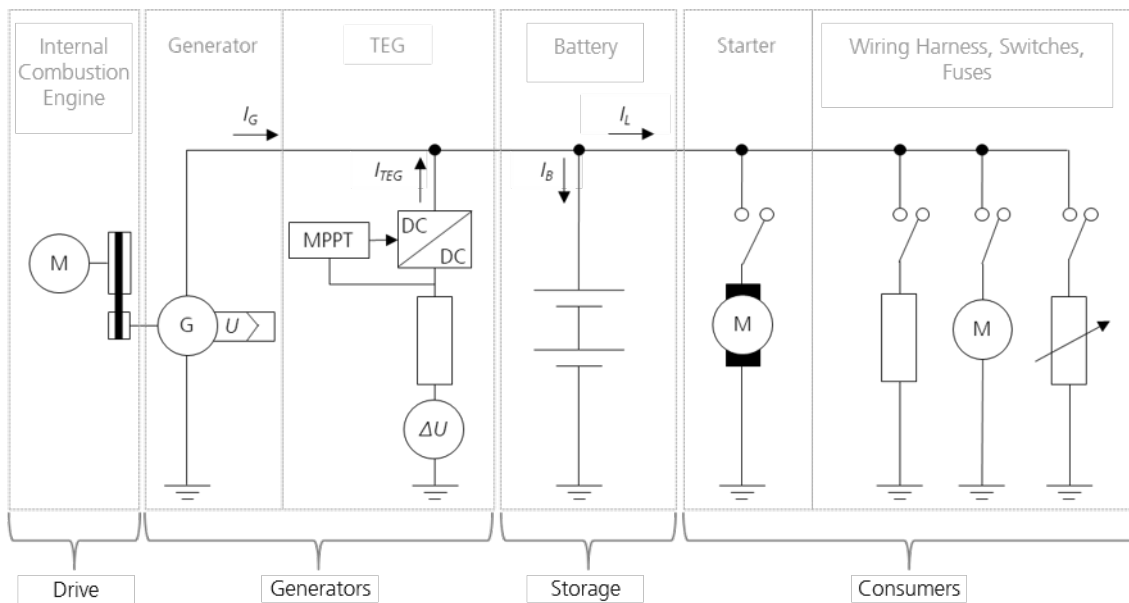


Figure 2-16 Illustration of the on-board electrical system of a conventional HDV with 24-volt on-board electrical system architecture

Evaluation of vehicle interactions

To evaluate the vehicle interactions of the TEG with the vehicle, all positive and negative (parasitic effects) interactions are summed to determine the change in fuel consumption of the vehicle (ΔB_e). For typical load points of a natural gas HDV for long-distance

transport, the vehicle interactions are balanced in Figure 2-17 as an example and summed to a resulting reduction in the fuel consumption.

Impact on the Internal Combustion Engine

- Additional mass m_{TEG} + 0,1 % ΔB_e^*
- Additional back pressure p_{TEG} + 0,05–0,3 % ΔB_e^*

+ Impact on the Cooling System

- Additional cooling load \dot{Q}_{TEG} 0 % ΔB_e^* (~ 40–90 kW)
- Additional pumping power P_{CP} < + 0,05 % ΔB_e^*

– Impact on the Electrical System

- Additional electrical power P_{TEG} –(0,8–2,3) % ΔB_e^*

= Sum: **–(0,35–2,1) % ΔB_e^***
($c=2,8–17,9$ g/km)

Figure 2-17 Example evaluation of the positive and negative effects of TEG integration in a natural gas HDV in terms of the change in fuel consumption (*for typical load points of highway travel; $B_e = 32.2$ kg/100 km; specific CO₂ emissions $c = 813$ g/km; TEG fully supplies the on-board electrical system)

2.5.2 Techno-economic boundary conditions

Within the scope of the project, the cost-benefit ratio was considered for the first time in the system optimization and minimized in such a way that the TEG system is economically viable and amortized in the natural gas HDV. For this purpose, knowledge of the total cost of ownership structure or, in the case of heavy-duty vehicles, the *Total Cost of Ownership* (TCO) and its dependencies is essential in order to incorporate them in the holistic simulation environment. As an objective of optimization, the lowest cost-benefit ratio is expected to be found that allows a minimum time of system amortization.

A total cost of ownership model for natural gas HDV with CNG and LNG refueling systems was created. For the latter, the cost allocation is shown in Figure 2-18 (a). In addition, target cost modeling was developed (see figure section (b)) that determines the benefit threshold and amortization for each TEG result design. The illustration shows the diesel HDV for comparison.

The following boundary conditions are defined as the deployment scenario and for evaluating the TEG system: Average annual kilometrage of the tractor unit of 150,000 km/year with a useful life of 5 years for the tractor unit or 10 years for the semitrailer.

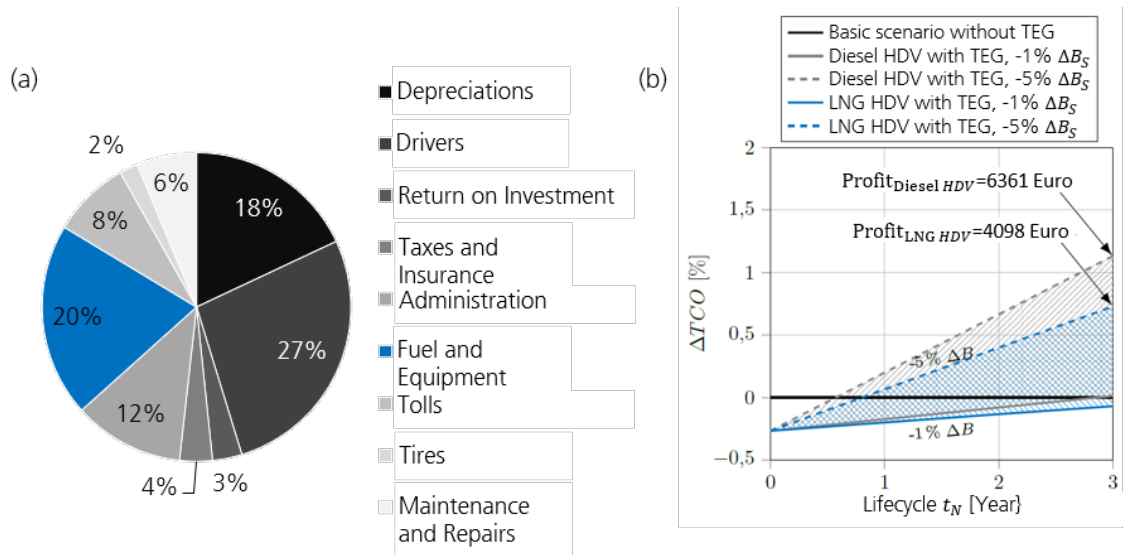


Figure 2-18 TCO cost structure for semitrailer truck with natural gas combustion engine (LNG) with kilometrage of 150,000 km/year (a) and target cost analysis of an example TEG design and indication of its benefit threshold (b; assumptions: Useful life of 5 years for the tractor unit or 10 years for the trailer, $B_s = 35.3$ l/100 km for the diesel or $B_e = 32.2$ kg/100 km or the natural gas HDV, TEG unit cost $K_{TEG} = 1500$ EUR)

2.5.3 Simulation environments and modeling

The Workbench from ANSYS Inc. is used, with the associated subroutines, as a basis of the simulation environment. The simulation environment is flexibly extendable and can also be linked to simulation and evaluation tools not available in ANSYS Workbench. The goal of the simulation environment described here is to simulate a TEG within the overall vehicle system, to mutually evaluate the vehicle interactions as well as the TEG system. This approach allows the holistic and simultaneous optimization of the heat exchanger and TEM to determine the optimal TEG design.

It is necessary to simulate its inner geometry in detail for the optimization of the heat exchangers and especially of the HGHEX. A corresponding CAD model was made in CATIA by Dassault Systèmes for this purpose. With the CadNexus bidirectional

interface, the possibility of combining the CAD model with the CFD model and thus allowing an iterative approach to optimization. This procedure is clarified in Figure 2-19.

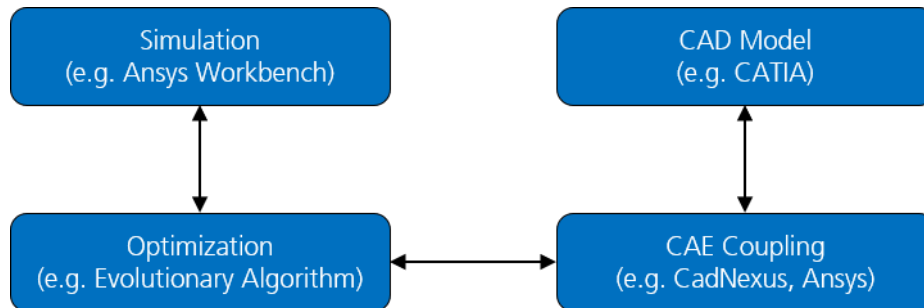


Figure 2-19 Integration of the CadNexus interface for bidirectional communication of the CAD model in CATIA and ANSYS Workbench

The challenge and complexity in creating and using such a CAE model environment is to ensure that all changes, including geometric changes, are update stable and automated in one iteration step.

As shown in the example form of the simulation environment in ANSYS Workbench in Figure 2-20, the geometry still has to be prepared for the CFD simulation. This is done through meshing. This must also be update stable to account for all changes in geometry and create an efficient mesh. The CFD simulation can only generate reliable and meaningful results with a high mesh quality. Only this complex procedure allows the calculation of a very high number of variants in a reasonable amount of time and the required multi-criteria optimization.

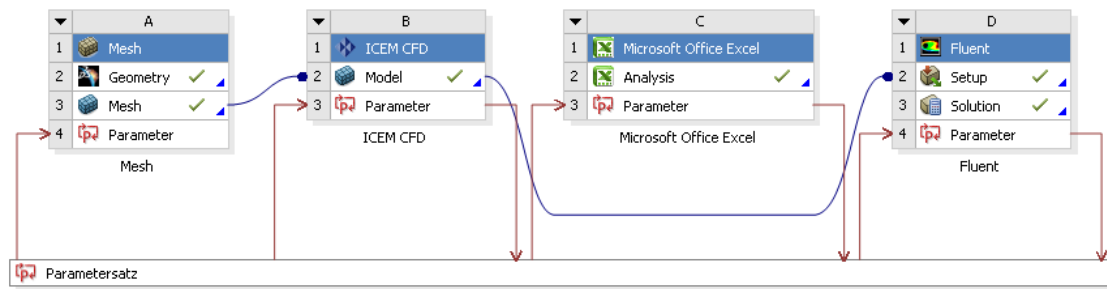


Figure 2-20 Example graphical user interface of the simulation environment in Ansys Workbench

Chapter 2.5.1 shows how the influences of the TEG affect the overall system. In order to use these findings in the simulation environment, a mathematical model is created and integrated into the simulation. Because of the structural design of ANSYS Fluent, it is possible to extend the calculations with self-made models and approaches using the C programming language.

Due to the physical dependencies of the existing data regarding the influences on the overall system, it was possible to interpolate these data with the help of a mathematical model. This mathematical model is then integrated into the simulation environment. This means that for any given boundary condition, such as speed or load, the resulting effect of the TEG on the overall vehicle system can be calculated and evaluated.

The additional weight of the TEG can thus be evaluated as an interaction, for example. For this purpose, as already introduced in chapter 2.5.1, a longitudinal dynamics simulation for HDV was created in order to evaluate the additional weight due to the TEG. These results were then transferred to the interpolated mathematical model, as exemplified in Figure 2-21. The procedure was analogous for the other positive and negative TEG effects.

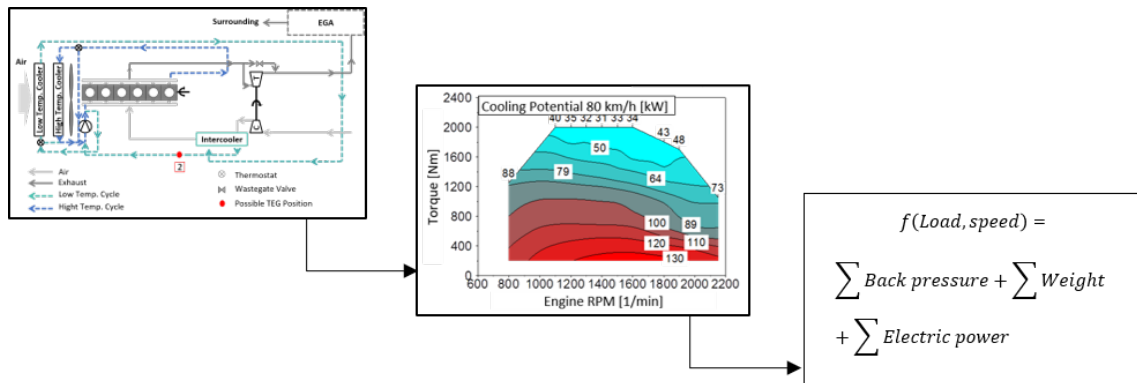
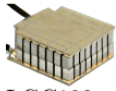
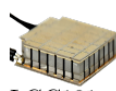



Figure 2-21 Example transformation from the physical replica using the simulation result via derivation into a mathematical model from the simulative results.

The thermoelectric modules used were developed and manufactured specifically for this application and according to DLR specifications by LG Chem Ltd (see Table 2-10). High temperature capable and efficient segmented TEM consisting of bismuth telluride (BiTe) on the cold side and skutterudite (SKD) on the hot side were used. Only the simultaneous optimization and adaptation of the TEM and the HGHEX will ensure that the required optimum – and, therefore, the lowest cost-benefit ratio – is achieved for the application.

Table 2-10 Overview based on the manufacturer's data of the investigated highly efficient and segmented TEM for high operating temperatures of LG Chem Ltd.

				
		LGC102	LGC101	LGC100
leg material	[-]	BiTe & SKD	BiTe & SKD	BiTe & SKD
max. temperature (shortterm)	[°C]	500 (550)	500 (550)	500 (550)
module dimensions	[mm]	31x31x5,2	31x31x4,4	31x31x3,2
leg height	[mm]	1,9 / 2	1 / 2	1 / 1
number of leg pairs	[-]	31	31	31
weight	[g]	25,4	19,7	14
electrical resistance ¹	[Ω]	0,2	0,2	0,1
max. power ²	[W]	14,7	18,6	26 (20,5)
max. efficiency ²	[%]	9	8,2	7,5

¹ At ambient temperature $\vartheta_a=25\text{ °C}$.

² At $\vartheta_{HS}=500\text{ °C}$ and $\vartheta_{CS}=50\text{ °C}$.

Preliminary experimental tests of the modules were carried out by the manufacturer and by DLR. Based on these measured data, an interpolation was performed to obtain the mathematical dependence of the temperature difference of the hot and cold side temperatures using the temperature difference ΔT and the corresponding efficiency or

electrical power. In this way, it was possible to derive characteristic maps as input variables for the TEG simulation environment. As an example, these are shown by means of a selected array of curves in Figure 2-22 based on the target selected TEM LGC100 (see equations (5) and (6) of chapter 5.1 in the Appendix). For the simulation environment, it is advantageous to capture and integrate the dependencies of the module data multidimensionally.

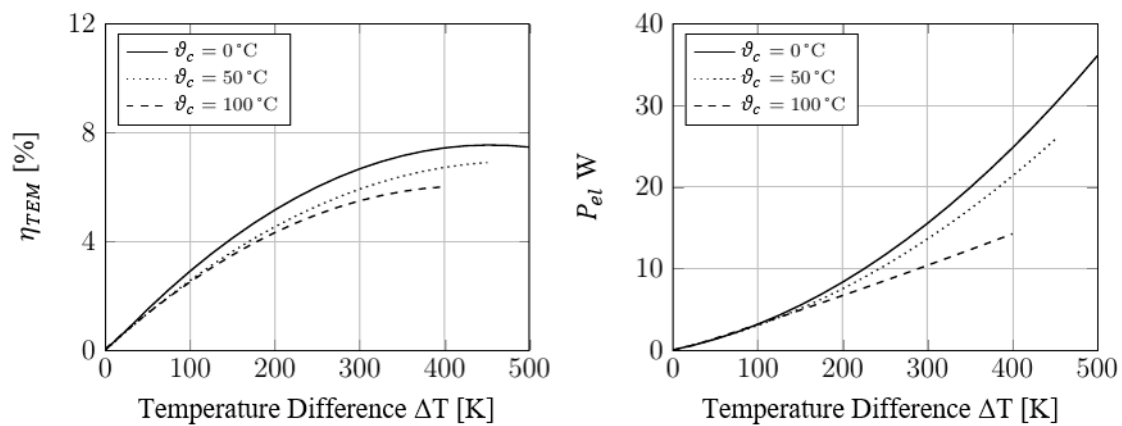


Figure 2-22 Module characteristics based on the module measured values of efficiency and electrical power of the selected TEM (LGC100)

When modeling the TEG, all the components already mentioned are brought together in a simulation environment. As already mentioned in chapter 2.5.3, a CAD model of the heat exchanger structure is used for the optimization. The geometry and complexity are reduced. The principle of periodicity is also utilized to keep model complexity and computation time as low as possible. A basic representation of the geometry of the CFD model is shown in Figure 2-23. The main flow direction of the exhaust gas is along the x-coordinate. Based on the reduced model structure, it is possible to make a statement about the overall system and its interactions.

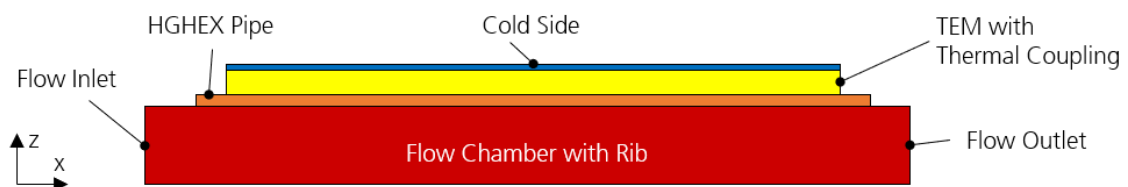


Figure 2-23 Schematic diagram of the CFD model of the model environment

For the correct and realistic modeling of the heat transfers, the thermal contacts used to reduce the contact resistances are also considered in the simulation. This allows the heat flow needed to calculate the electrical power through the TEM to be calculated correctly.

The TEM is integrated as a substitute model into the simulation. The corresponding material properties of the components are implemented as a function of temperature. Despite the simplification made and the efficient approach, it is still possible to correctly model the heat flow as well as the resulting electrical power. This could be demonstrated, among other things, with the help of the validation study from chapter 2.4.2 and the simulation environment could thus be verified.

2.5.4 Simulation results

Due to the simulation environment described in the previous chapters, the developed methods and partial models, it was now possible to generate simulation results under the given boundary conditions. As a reference, on-board operating points were defined in chapter 2.2. These enable the TEG result designs achieved to be evaluated in the part-load range, but also in the high-load range, in different application profiles.

The complexity in selecting the optimum is to be explained using the preliminary investigation on the TEG length and the result variable of the backpressure Δp . Figure 2-24 shows the ratio of the expected electrical power of each result design to the backpressure. The result designs were split based on TEG length in flow direction. Here, the number of TEMs in the flow direction has been discretized and is of relevance. It varies here from 2 to 5 TEM strips in the direction of flow. The total number of TEMs remains the same, however, as does the module area. But the ratio of the TEG length in the flow direction to the TEG width differs. Fluid mechanically, a wider TEG – just like a higher TEG – means lower flow velocities. A longer TEG, with otherwise identical geometry, will have a higher backpressure but also a higher heat flow. To find the optimum for the TEM area, a rough optimization was performed with respect to the length of the TEG in the flow direction.

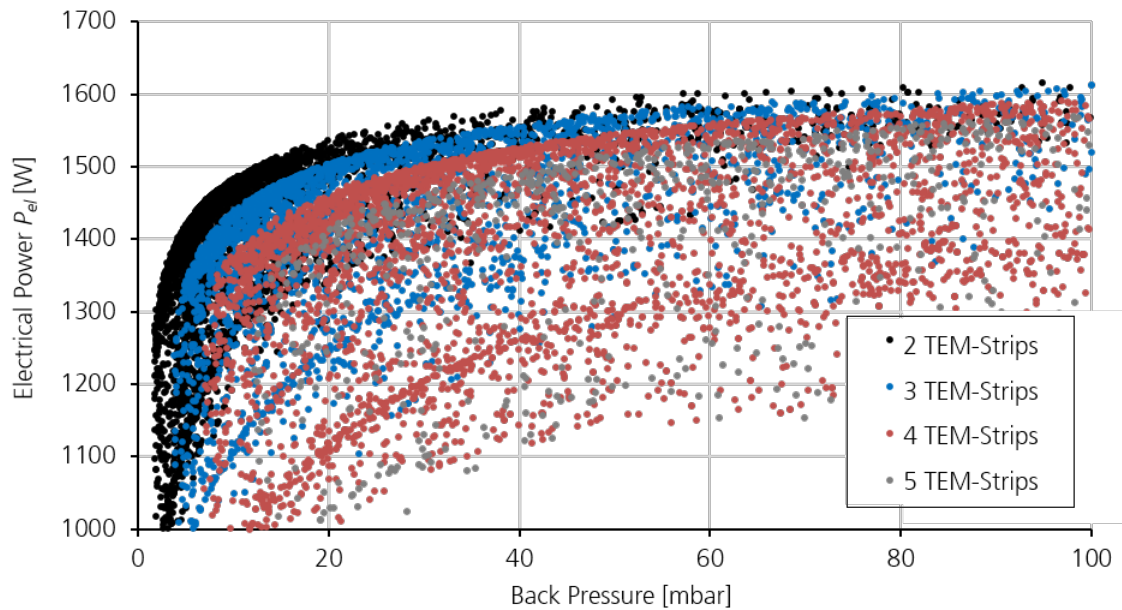


Figure 2-24 Results of the preliminary investigation on the influence of the TEG length in the flow direction

It was found that, with a shorter TEG, the expected electrical power increases compared to a longer one, and this at a lower backpressure level. This result confirms the assumption made earlier and can be explained by the higher thermoelectric efficiency. With a short but wide TEG geometry, the average temperature difference between the hot and cold sides is higher. This increases the thermoelectric efficiency, and thus the maximum electrical power that can be expected. By keeping the module area the same in this optimization, a shorter TEG also means a wider TEG. This means the lower flow velocities provide a comparatively low backpressure. No final holistic balance or cost-benefit ratio has yet been calculated in this preliminary study. As a conclusion, it can nevertheless be stated that the positive effect due to a higher output line for a TEG with 2 TEM strips in the direction of flow is offset by a very complex, heavy and expensive design due to the effective total width of more than 750 mm (see geometric boundary conditions from chapter 2.2). In this case, an optimal compromise between a high resulting positive effect on the overall system and a feasible and, above all, economically justifiable design lies with a TEG with 3 TEM strips in the direction of flow.

The selection of a weighted optimum of the holistic simulation environment, in which all negative and positive effects on the overall system were balanced and a cost-benefit ratio was calculated, was more complex. In the multicriteria optimization, a weighting of

the result variables was carried out. A TEG with 3 HGHEX, 4 COHEX and 144 TEM LGC100 was identified as the target TEG result design. This is characterized by calculated system costs (assuming a high volume production) of 1002 EUROS, a weight of 27.4 kg and a heat exchanger area of 1655 cm². As a final summary of the TEG interpretation, please refer to Table 2-11. This shows all defined operating points with the final results achieved. The TEG electrical power P_{TEG} represents the electrical power of the TEM P_{el} multiplied by the power electronics efficiency η_{PE} . TEG integration takes place on the exhaust gas side directly after the EGA and as described in the LT CC.

The highest relative reduction in fuel consumption $\Delta B_{e,net}$ (resulting fuel consumption change after deduction of negative effects) was achieved with 2.5 % in OP 1.1, therefore in WHVC with 15 t TW on average. This was also the first time in the world that an amortization period of < 2 years was achieved for the TEG system, taking into account the assumptions of the TCO model. An amortization period of less than 3 years was achieved at all operating points. The minimum was determined to be up to one year in the average of the WHVC 40 t TW. The reduction as an absolute figure is up to 1 kg/100 km.

Further presentation of results for the dynamic simulation of the TEG power and the respective motor power in the respective WHVC are shown in the Appendix in Figure 5-13 and Figure 5-14. In the real SHHS distance, the available battery capacity is not large enough to store the excess TEG power in the drive time. If additional capacity were available, fuel reduction could be further increased.

Table 2-11 Result of the optimization of holistic TEG system design (TEG result design selected for maximum reduction of fuel consumption at most favorable system cost balanced over all operating points, OP)

OP	1.1	1.2	2.1	2.2	3.1	3.2	
Designation	WHVC _{15 t,m}	WHVC _{15 t,max}	WHVC _{40 t,m}	WHVC _{40 t,max}	SHHS _{40 t,m}	SHHS _{40 t,max}	
Vehicle	Fuel consumption (kg/100 km)	25.0	30.5	42.7	38.1	35.0	88.9
	Speed (km/h)	40.2	83.2	39.3	86.8	74.9	72
	Engine power (kW)	42	130	77	180	114	341
	Speed (rpm)	1106	1237	1119	1293	1392	1760
	Torque (Nm)	329	1003	587	1333	759	185
	Power P_{TEG} (W)	1030	1954	1424	2371	1686	2688
TEG system	Fuel consumption $\Delta B_{e,gross}$ (%)	-2.6	-1.7	-2.3	-1.9	-2.2	-1.4
	Fuel consumption $\Delta B_{e,net}$ (%)	-2.5	-1.5	-2.3	-1.6	-2.1	-0.8
	CO ₂ emissions (g/km)	-15.7	-11.6	-24.6	-15.5	-18.9	-18.0
	Weight m_{TEG} (kg)	27.4	27.4	27.4	27.4	27.4	27.4
	Costs C_{TEG} (EUR)*	1002	1002	1002	1002	1002	1002
	Amortization t_A (years)*	1.8	2.9	1.0	1.9	1.4	1.5

* Assumptions: Annual kilometrage 150,000 km, useful life 5 years, TEG system cost for large numbers (30,000 units/yr – experience curve effect: Consideration of costs in relation to the cumulative production volume).

2.6 WP 6: Validation through functional models

To validate the simulation results, two functional models were built to replicate the thermal heat flows and TEG design, as well as the determined TEG performance of the simulation. Both realizations, see Figure 2-25, deviate only slightly from the determined geometric TEG result design to minimize TCO. In the first functional model "HDTEG1" (see Figure 2-25 (a)), ceramic substitute modules, half mullite and half zirconia, with similar thermomechanical properties to the TEM were used. In the second setup "HDTEG2"¹, the TEM LGC100 from LG Chem (see Figure 2-25 (b)), with otherwise identical setup, were integrated.

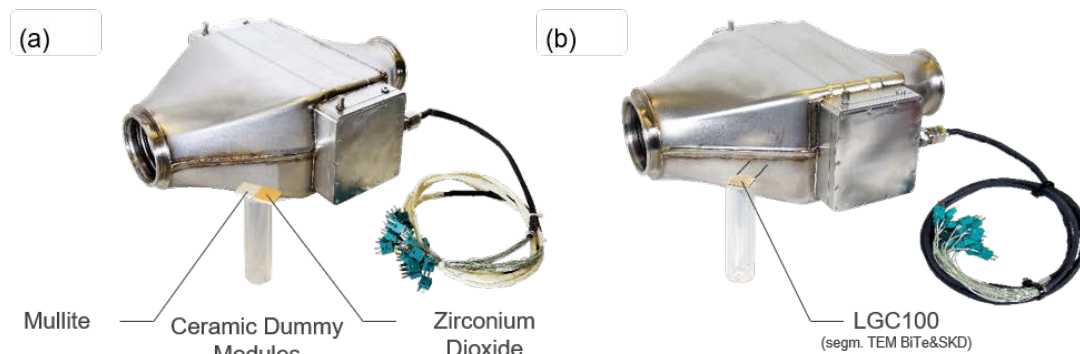


Figure 2-25 TEG functional model as hardware realization of the TEG result design with minimum TCO objective: (a) HDTEG1: Setup with spare modules and (b) HDTEG2: Setup with TEM LGC100 from LG Chem

The functional models were successfully tested experimentally on DLR's own hot gas test rig. The propane gas burner with maximum rated power of 200 kW (60 % of the rated power of the reference vehicle) enables the combustion engine to be simulated. Due to the lower power class than that of the HDV engine, the maximum load point in the SHHS reference route (SHHS_{40 t,max}) could not quite be reached. The cooling system of the heavy-duty vehicle was represented in the experimental setup with the aid of a sufficiently large temperature control unit. The on-board electrical system was mapped by a multiple maximum power point tracker (MPPT) including a DC-DC converter and two lead-acid batteries analogous to the on-board electrical system topology with 24-V

¹ The implementation of the second functional model "HDTEG2" was only made possible by additional financing or follow-up financing from DLR Technology Marketing.

voltage level and 220 Ah capacity. Figure 2-26 represents the principle hot gas and coolant flow routing in the TEG core. In addition, the test rig setup on DLR's own hot gas burner test rig can be found in the Appendix in Figure 5-15. The experimental setup thus corresponds to realization at technology maturity level 5: Test setup in operational environment.

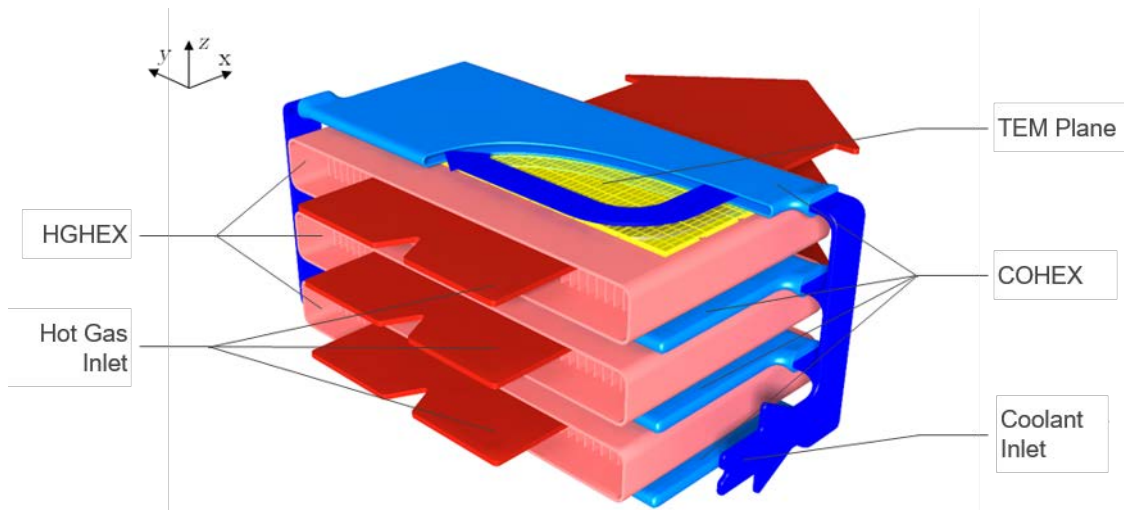


Figure 2-26 Schematic diagram of the TEG functional pattern in counterflow design based on the TEG core (without housing components) and the hot gas and coolant flow paths

Table 2-12 lists the results of the functional model HDTEG2 on the basis of the temperature difference present at the respective operating point and the resulting electrical generator output. In general, good agreement between simulation and experiment is evident, especially with respect to generator performance. As an average value, the deviation is only -2% . Up to 2562 W could be measured at the peak load point OP3.2. For the average surface temperatures of the heat exchangers, the difference between simulation and experiment is larger when considering the absolute deviations. As an average value, the deviation across all operating points is 2.2%. 60 sheath thermocouples were inserted into the surfaces to record temperatures at specific points. The mean values were determined from these measurement data. Each temperature sensor is subject to a different measurement deviation that already leads to deviations. In addition, inhomogeneous temperature distributions occur in each COHEX and HGHEX and across the respective flow direction. Both are not represented by the simulation, which can already explain the deviations in the indicated range. In addition, the simulative mapping of the thermal resistance change of the TEM during current flow

caused by the influence of the Peltier effect is complex and was neglected due to its relatively small influence.

Table 2-12 Comparison of the average hot $\bar{\vartheta}_{HS}$ and cold side temperatures $\bar{\vartheta}_{CS}$ as well as the electrical generator output P_{TEG} between the simulation and the experiment of the HDTEG2 functional model on the hot gas test rig

OP*		1.1* ²	1.2* ²	2.1* ²	2.2* ²	3.1* ³	3.2* ⁴
Designation		WHVC _{15 t,m}	WHVC _{15 t,max}	WHVC _{40 t,m}	WHVC _{40 t,max}	SHHS _{40 t,m}	SHHS _{40 t,max}
Average hot side temperature $\bar{\vartheta}_{HS}$	Simulation	299.6 °C	437.7 °C	390.5 °C	493.7 °C	432.3 °C	512.1 °C
	Experiment	315.7 °C	438.1 °C	394.2 °C	486.4 °C	439.3 °C	518.2 °C
	Deviation	5.4%	0.1%	0.9%	-1.5 %	1.6%	-2.6 %
Average cold side temperature $\bar{\vartheta}_{CS}$	Simulation	53.1 °C	75.9 °C	67.6 °C	81.6 °C	73.6 °C	90.5 °C
	Experiment	57.3 °C	79.4 °C	69.8 °C	81.8 °C	78.1 °C	90.6 °C
	Deviation	7.9%	4.5%	3.2%	0.3%	6.1%	0.1%
Power P_{TEG}	Simulation	1163 W	2013 W	1592 W	2445 W	1987 W	2664 W
	Experiment	1118 W	1954 W	1657 W	2365 W	1957 W	2562 W
	Deviation	-4 %	-3 %	3.9%	-3.4 %	-1.6 %	-4 %

* The measurement deviation is not indicated for better clarity of the results.

*² deviation from Table 2-6: $\vartheta_{LT\ CC,in}=20\text{ °C}$, $\dot{v}_{LT\ CC}=0.4\text{ dm}^3/\text{s}$.

*³ deviation from Table 2-6: $\vartheta_{LT\ CC,in}=20\text{ °C}$, $\dot{v}_{LT\ CC}=0.5\text{ dm}^3/\text{s}$.

*⁴ deviation from Table 2-6: $\vartheta_{LT\ CC,in}=20\text{ °C}$, $\dot{v}_{LT\ CC}=0.5\text{ dm}^3/\text{s}$, $\dot{m}_{Ex}=906\text{ kg/h}$.

The temperature distribution in the flow and longitudinal direction to the heat exchanger is exemplified in Figure 2-27 for OP1.1 and OP3.2. This again shows the good correlation between simulation and experiment as well as the mentioned deviation of the measured values in the individual heat exchangers. The measured values of the cold side are generally higher than the simulated values. For the hot side, this deviation is only evident in the middle of the HGHEX in OP1.1*. The good comparative uniformity in the longitudinal direction should be emphasized, and can be expressed quantitatively as temperature drop per length HGHEX in OP1.1* with 11.7 °C/cm and in MP3.2* with only 4.6 °C/cm.

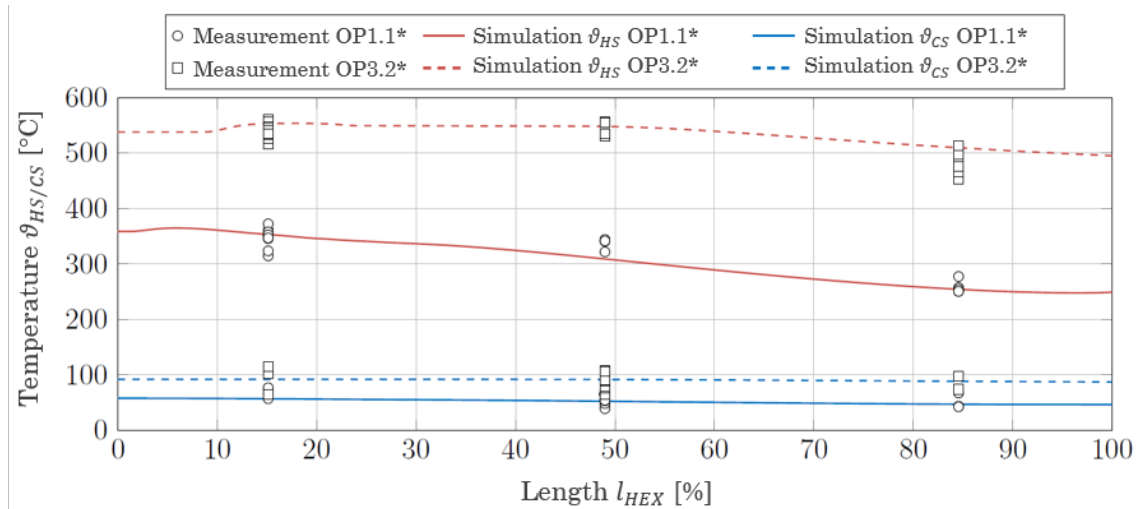


Figure 2-27 Comparison of the hot and cold side temperatures between the simulation and the experiment of the functional model HDTEG2 on the hot gas test rig at operating points 1.1* and 3.2** (*: For boundary conditions, see Table 2-12)

The comparison between simulation and experiment of the TEG backpressure for all operating points can be found in Table 5-4 in the Appendix. Here, the simulation values could be confirmed with a low average deviation < 6 %. In addition, the reproducibility of the measured values by both HDTEG1 and HDTEG2 function samples that are identical in construction should be emphasized. The level of backpressure is typically selected to be very low for components in heavy-duty vehicle exhaust systems in order to minimize this parasitic effect.

Due to the predominantly good to very good (mostly > 90 %) correlations between simulation and the experiments, the holistic simulation environment is considered validated. Very high TEG performances compared to the state of the art (see Table 2-3) could also be confirmed in experiments. Using the TEG core, which weighs about 15.5 kg and has a volume of just 8.3 dm³, a power density of the TEG system of up to 174 W/kg and 326 W/dm³ can be determined on the basis of the experimental measured values. These key figures represent global technology peaks for TEG systems in heavy-duty vehicles.

2.7 WP 7: Evaluation and outlook

2.7.1 TEG potential assessment and outlook

The achieved project results of the TEG design for an innovative natural gas HDV can be considered as very successful, as all objectives of the project, which were initially formulated in a very challenging way, could be achieved. For the first time in the world, an amortization period of < 2 years was achieved for the TEG system for HDV. It was also possible for the first time to demonstrate that TEG systems can be used economically in HCVs with natural gas engines. Compared to the state of the art, an increase of up to 440 %, based on the comparison of TEG performance, could be achieved for a TEG system in natural gas HDVs compared to the work of Hervas-Blanco et al. [11], an increase of up to 440 %, based on the comparison of TEG performance, was achieved for a TEG system in a natural gas HDV. It is noteworthy that especially the system costs and the additional weight were taken into account in the present project in contrast to the work of Hervas-Blanco et al.

A conventional heavy-duty vehicle was used as the basis for evaluation in this project. As a future potential, the electrification of auxiliary units, for example, would further increase the benefit of the TEG system, especially on the real driving route, as this would increase the electrical consumer demand. According to initial estimates, this would allow at least a further 0.5 percentage points of fuel reduction to be achieved in addition to the results already listed. It is expected that both thermoelectric materials and modules as well as heat exchangers will be able to deliver even better efficiencies and performance figures in the future. For example, just increasing the efficiency of the semiconductor material used in the TEM by 25 % compared to the one used in this project would increase fuel reduction by up to a further 0.7 percentage points. If it becomes possible to bring this promising technology to production maturity following this project, significant cost reductions can also be expected.

2.7.2 Outlook of future HDV engines with regard to waste heat utilization

In order to achieve the climate targets in the Paris Agreement, the EU Parliament had decided to reduce CO₂ emission values from heavy-duty commercial vehicles 30 % by 2030. The dramatic tightening of CO₂ poses a very significant challenge to the

development of technology for heavy-duty vehicles. In modern internal combustion engines, more than 50 % of the energy released by the fuel injected into the cylinders is emitted unused into the environment. Figure 2-28 shows a Sankey diagram for the distribution of the primary energy used in the internal combustion engine as an example.

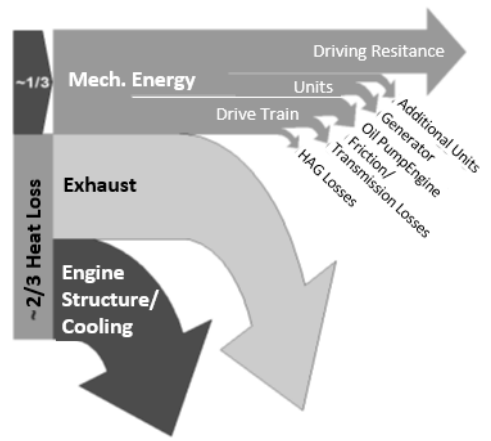
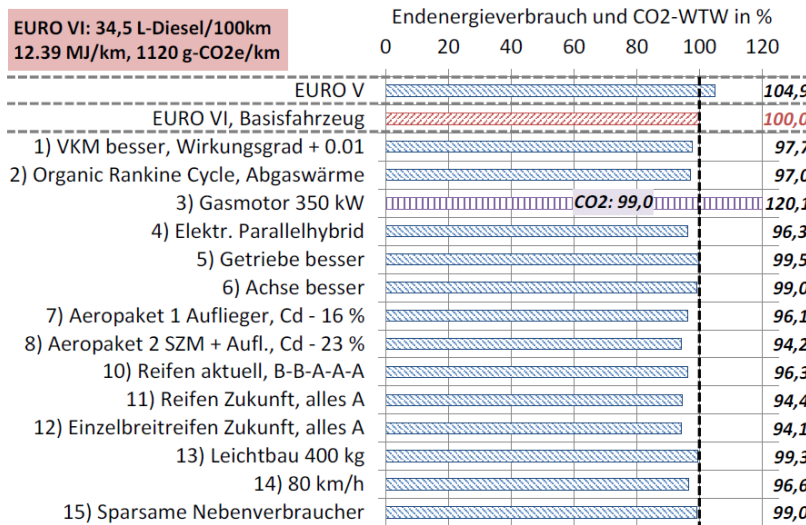


Figure 2-28 Breakdown of primary energy used in the internal combustion engine [12]

Based on this fact, residual heat recovery technologies based on different approaches, such as the Seebeck effect (thermoelectric generators, TEG), Rankine process (ORC) and turbocompound, may well contribute in achieving the stricter regulatory requirements for CO₂ emissions.

Future heavy-duty vehicles will be optimized with extensive new technologies. Different future measures for increasing the efficiency of heavy-duty commercial vehicles were compared in a study [10] by the Federal Environment Agency. The VECTO simulation software was used to realize the potential analyses. Figure 2-29 shows the potentials of CO₂ reduction of the selected future technologies for heavy-duty commercial vehicles



Die dargestellten Balken zeigen den geänderten Endenergieverbrauch. Wo aufgrund des Einsatzes alternativer Energieträger (statt Diesel) die Änderung der Treibhausgasemissionen (CO₂-Äquivalente well-to-wheel) von der Änderung des Energieverbrauchs abweicht, sind entsprechende Zahlenangaben separat ausgewiesen.

Figure 2-29 Semitrailer on *Long Haul Cycle*, individual measures [10]

Figure 2-30 shows the analysis results of the study for the changes in the vehicle costs of a semitrailer with 40 t TW in long-distance transport.

With regard to the application of residual heat utilization technology, two principles can generally be followed in the optimization of the heavy-duty vehicle engine. With the first principle, the energy balance of the engine can be optimized or adjusted in such a way that the waste heat into the coolant is reduced, and the exhaust gas heat is increased in return. One example is the use of a new generation of piston coatings in heavy-duty vehicle diesel engines. Mahle presented the technology in [13]. In addition, thermal management can be optimized to provide more cooling potential of the cooling system for residual heat recovery systems. An example of this is presented in the publication from Mahle [14].

Reducing CO₂ emissions for heavy-duty commercial vehicles by 30 % by 2030 is a major challenge. Achieving these target values is only ever possible with a combination of technologies, e.g. use of CNG/LNG aerodynamic measures and residual exhaust gas heat utilization. In such combinations, a TEG can have a good cost-benefit ratio, and it is possible to reduce a vehicle's CO₂ emissions by 30 %.

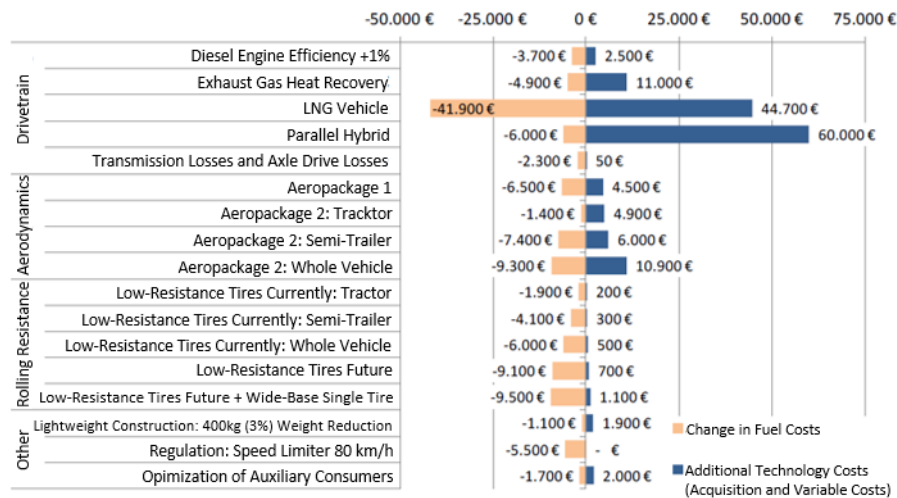


Figure 2-30 Change in vehicle costs of a 40 t semitrailer in long-distance transport by 2018 [10]

This will not be sufficient to achieve the CO₂ fleet targets, however, as diesel drives will foreseeably be sold in 2030 as well and will be included in the fleet emissions with higher CO₂ emissions. As it is not foreseeable what fleet proportions of fuel cell drives (with hydrogen: H₂) will be available by 2030, the use of hydrogen in internal combustion engines is also currently in focus again. Since the oxidation catalyst and particulate filter are no longer required in the exhaust gas aftertreatment system there, the installation situation for a TEG will be improved. It is difficult to estimate the temperature boundary conditions for a TEG in an H₂ engine. In principle, hydrogen initially leads to significantly hotter combustion, but this is generally compensated or overcompensated by a strong mixture dilution. The degree of mixture dilution results from the design of the overall engine. In principle, however, it can be assumed that there should also be great potential for waste gas heat utilization in H₂ combustion. The project results show great potential for thermoelectric technology to increase efficiency in the natural gas engine under study. In addition, the promising results also point to a worthwhile application in diesel engines and for the combustion of hydrogen and other synthetic, regeneratively produced fuels.

3 Reflection

At the end of the project, the work was documented according to the original project description in WP 1 to WP 7. Partial results were already presented in Interim Reports I and II and are therefore not listed again in detail. All reports and work packages have been summarized in this final report.

The achieved project results of the TEG design for an innovative natural gas HDV can be fully evaluated as positive. The efficiency of modern heavy-duty commercial vehicles through the use of a new type of waste heat recovery system in the form of a TEG could be demonstrated simulatively and by means of realized functional models. Fuel reduction of up to 2.5 % was simulatively determined and system amortization was achieved in < 2 years. Depending on the driving scenario and the load points, this is already within the realm of possibility after one year. In the process, a heavy-duty vehicle-specific TEG system was developed for the first time with the help of a holistic development approach and the potential of this technology for current and future heavy-duty vehicles (further +1.2 percentage points, fuel reduction up to 3.7 %) was presented. In the project, a highly integrated TEG design for heavy-duty vehicle applications was developed and realized for the first time, as it offers many advantages for potential series production as well as improving the state of the art in many respects. During the hardware implementation in the form of a functional model, more than 2.5 kW of electrical power was measured, which corresponds to 98 % of the simulation values and thus a good agreement with the simulation.

The close cooperation of project partners DLR FK and FKFS in the system development made it possible to achieve these advances and to design the TEG specifically for the advantages and requirements of the reference vehicle. The selected approach made it possible to optimally utilize the expertise, focal points and technical orientations of the participating research institutions. The intensive cooperation also further improved the networking between the institutes.

We would like to take this opportunity to thank the Baden-Württemberg Ministry of Economics, Labor and Housing for supporting and funding the project. It is thanks to DLR Technology Marketing that follow-up funding made it possible to realize the hardware of the second functional model, fully equipped with TEM, on a scale of 1:1. In

In addition, thanks are due to LG Chem which provided the thermoelectric modules as part of a collaboration with the DLR Institute for Vehicle Concepts and relied on its expertise in TEG design. Thanks are also due to the support and expertise of all the other partners and companies involved, especially in Baden-Württemberg.

The knowledge gained in this project is intended to serve as a solid basis for future projects in the automotive industry, to strengthen Germany as a research location, and to serve Baden-Württemberg's pioneering role in innovation in the automotive sector.

In summary, the project was able to develop a novel thermoelectric generator for an innovative natural gas heavy-duty vehicle. In-depth scientific knowledge was gained in the overall system, the system design of the TEG and the design of the thermoelectric module component. These have resulted in numerous publications (see chapter 2.0). The processing of the project showed that there is enough potential for a continuation of the project or task. The results of the project will help thermoelectrics on its way into vehicles.

4 Bibliography

- [1] Lastauto Omnibus, "Messfahrten 1967–2012," *Lastauto Omnibus*, 04/2014.
- [2] Bundesministerium für Verkehr, Bau und Stadtentwicklung, 03 08 2017. [Online]. Available: https://www.bmvi.de/SharedDocs/DE/Anlage/MKS/mks-strategie-final.pdf?__blob=publicationFile.
- [3] LNG Blue Corridors, "Demonstration of heavy duty vehicles running with liquefied methane," 03 08 2017. [Online]. Available: <http://lngbc.eu/>.
- [4] C. Stiewe and E. Müller, "Anwendungspotential thermoelektrischer Generatoren in stationären Systemen – Chancen für NRW: Studie im Auftrag des Ministeriums für Innovation, Wissenschaft und Forschung des Landes Nordrhein-Westfalen," Deutsches Zentrum für Luft- und Raumfahrt e. V., Köln, 2015.
- [5] L. Olsson and B. Andersson, "Kinetic Modelling in Automotive Catalysis.," *Topics in Catalysis*, April 2004.
- [6] Holger, Bollig, Anderson and Hochmuth, "A discussion of transport phenomena and three-way kinetics of monolithic converters," *Chemical Engineering Science*, 2006.
- [7] C. Häfele, "Entwicklung fahrzeuggerechter Thermoelektrischer Generatoren zur Wandlung von Abgaswärme in Nutzenergie," Deutsches Zentrum für Luft- und Raumfahrt e. V., Forschungsbericht DLR 2016-08, Köln, 2016.
- [8] C. Hagelüken, *Autoabgaskatalysatoren*, Renningen: Expert Verlag, 2016.
- [9] VECTO, "Standarddaten 07/2014," 2014. [Online]. Available: https://ec.europa.eu/clima/policies/transport/vehicles/vecto_en. [Accessed 18 08 2018].

- [10] F. Dünnebeil, C. Reinhard, U. Lambrecht and A. Kies, "Zukünftige Maßnahmen zur Kraftstoffeinsparung und Treibhausgasminderung bei schweren Nutzfahrzeugen," *Studie Umwelt Bundesamt*, 04 2015.
- [11] E. Hervas-Blasco, E. Navarro-Peris, M. Rosa and J. Corberán, "Potential fuel saving in a powertrain derived from the recovery of the main energy losses for a long haul european mission," *Energy Conversion and Management*, no. 150, p. 485–499, 2017.
- [12] J. Liebl and A. Eder, "Wärmemanagement - ein Beitrag zu BMW Efficient Dynamics.," *Wärmemanagement des Kraftfahrzeugs VI.*, 2008.
- [13] Mahle, "Kolbenbeschichtung," *MTZ*, 12 2018.
- [14] R. Lutz, A. Kleber and E. Pantow, "Potentialuntersuchung zur indirekten Ladeluftkühlung bei Nutzfahrzeugen," *Ladungswechsel im Verbrennungsmotor*, 2016.

5 Appendix

5.1 Equations

- Heat convection, i.e. the transfer of heat by entrainment in moving media or flows, is described via the heat flow \dot{Q} :

$$\dot{Q} = \dot{m}c_p\Delta T = \dot{m}c_p(\vartheta_1 - \vartheta_2) \quad (1)$$

\dot{m} represents the mass flow, c_p the specific heat capacity of the medium at constant pressure and ΔT the temperature difference as well as ϑ_i the respective temperatures.

- The exergy flows \dot{E} are determined by multiplying the heat flux by the Carnot efficiency n_c :

$$\dot{E} = \dot{Q}n_c = \dot{Q}\left(1 - \frac{T_c}{T_h}\right) \quad (2)$$

Carnot efficiency represents the highest possible theoretical efficiency in the conversion of thermal energy into mechanical energy, taking into account the temperature of the heat source T_h or the heat sink T_c . It is meaningful for qualitative assessment, but has little practical value quantitatively.

- Carnot efficiency is only true if the temperature of the heat source and sink remains constant, which is not usually the reality. In a TEG-based waste heat recovery system, the heat source experiences a temperature drop during the heat exchange process while the heat sink is heated. The more realistic triangular process efficiency n_{Dr} can be introduced for this:

$$n_{Dr} = 1 - \frac{\ln\left(\frac{T_h}{T_c}\right)}{\frac{T_h}{T_c} - 1} \quad (3)$$

- Nevertheless, high-temperature and low-temperature circuits are available for integrating the TEG into the engine cooling system. The heat dissipation from

the TEG into the cooling circuit can be calculated in principle with the following equation.

$$\dot{Q}_{CO,potential} = c_{p,CO} \cdot \dot{m}_{CO} \cdot (T_{CO,out} - T_{CO,in}) \quad (4)$$

$\dot{Q}_{CO,potential}$ is the maximum amount of heat that may be fed into the cooling system. $c_{p,KM}$ is the specific heat capacity of the coolant. \dot{m}_{CO} is the mass flow of the coolant. $T_{,out}$ and $T_{,in}$ are temperatures of the coolant at the inlet or outlet from the heat supply point. $c_{p,CO}$ depends on the coolant temperature and is calculated in GT-Power by fitting a polynomial. $T_{,in}$ depends both on the integration position of the TEG in the cooling system and on the other heat sources in the cooling system, such as the combustion engine and intercooler.

- The electrical power P_{el} of one or more thermoelectric modules is determined by the module efficiency η_{TEM} and the amount of heat flow \dot{Q} [W] from the hot to the cold side:

$$P_{el} = \eta_{TEM} \cdot \dot{Q} \quad (5)$$

- The efficiency, assuming the maximum output power, can be described in terms of the figure of merit Z , the hot T_h and cold side temperatures T_c , and their average temperature $\bar{T} = \frac{T_h + T_c}{2}$ as:

$$\eta_{TEM} = \eta_c \cdot \frac{1}{\frac{4}{Z \cdot T_h} + 2 - \frac{1}{2} \frac{T_h - T_c}{T_h}} \quad (6)$$

5.2 Additional results

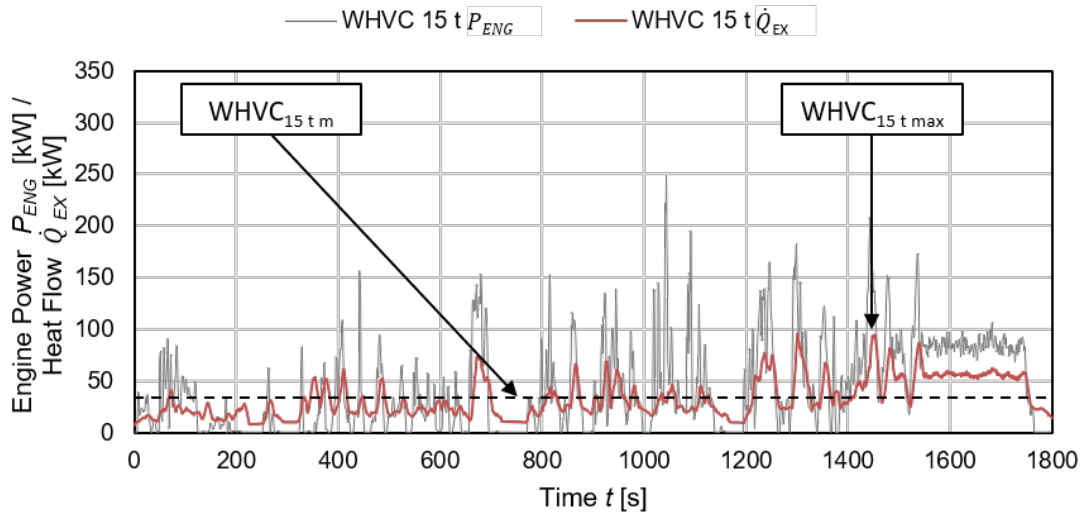


Figure 5-1 Result of the potential analysis based on the engine power and the available exhaust enthalpy in the EGA for the natural gas HDV in the WHVC with 15 t TW

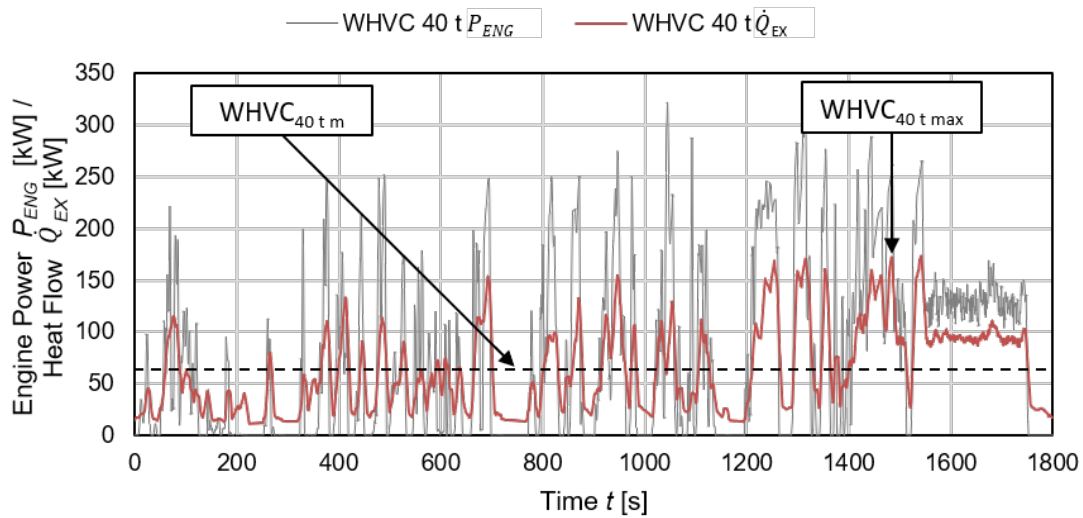


Figure 5-2 Result of the potential analysis based on the engine power and the available exhaust enthalpy in the EGA for the natural gas HDV in the WHVC with 40 t TW

Table 5-1 Technical data of the research engine, Cursor 13 gas engine

Variables	Unit	Values
Nominal power P_{nom}	[kW]	338 @ 1900 rpm
Max. torque M_{max}	[Nm]	2000
Piston stroke h	[mm]	150
Bore d_B	[mm]	135
Displacement V_d	[L]	12.9
Geom. compression ratio ϵ_{geo}	[-]	12:1
Number of valves (inlet valves/outlet valves)	[-]	4 (2/2)

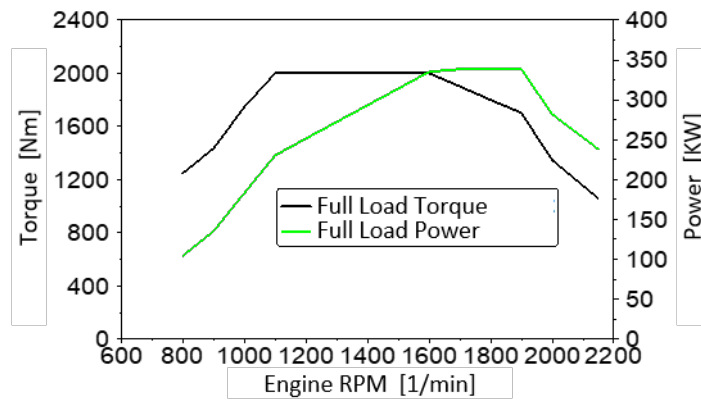


Figure 5-3 Full load curve of the Cursor 13 gas engine

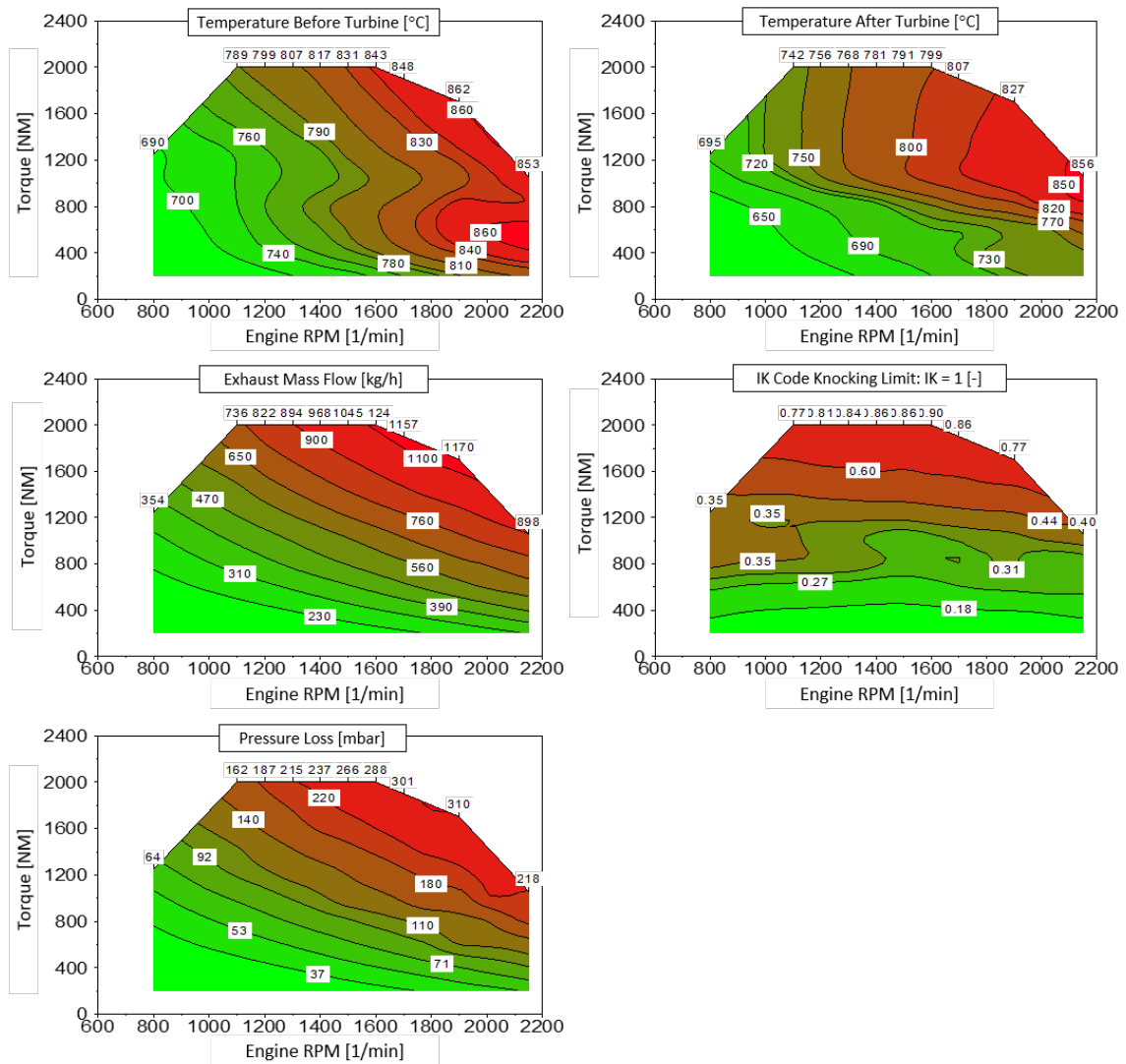


Figure 5-4 Simulation results for exhaust gas temperatures and mass flows, I_K value, pressure losses in the three-way catalytic converter as a function of engine speed and torque

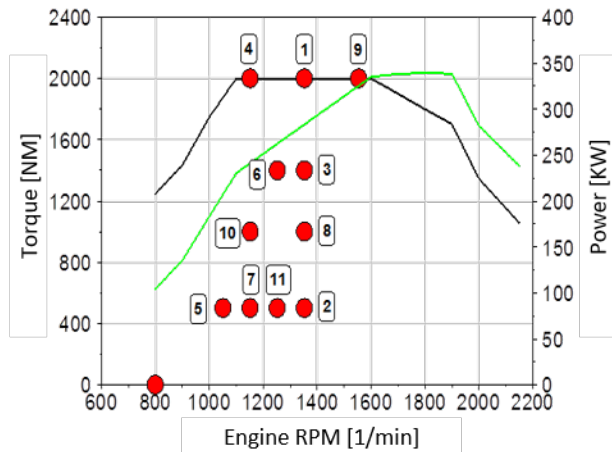


Figure 5-5 WHSC operating points

Operating Point (OP)	RPM [1/min]	Torque [NM]
1	1353	2000
2	1353	500
3	1353	1399
4	1152	2000
5	1052	500
6	1253	1399
7	1152	500
8	1353	1000
9	1555	2000
10	1152	1000
11	1253	500
Idle	800	0

Table 5-2 WHSC operating points

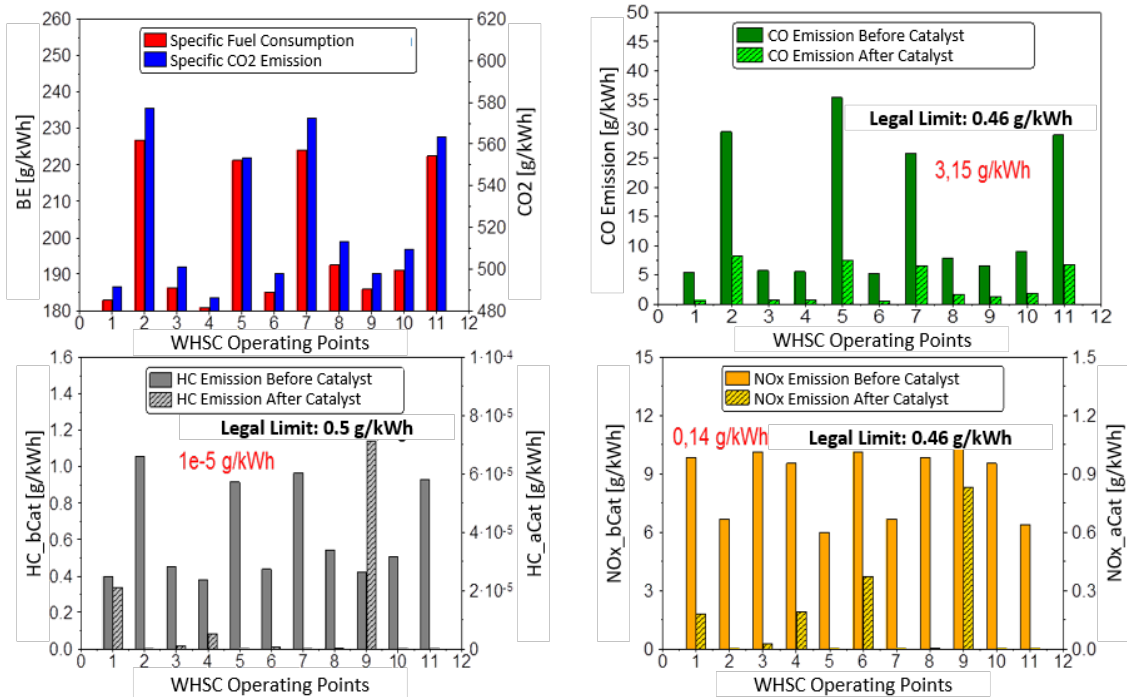


Figure 5-6 Simulation results for specific fuel consumption and exhaust emissions in WHSC operating points

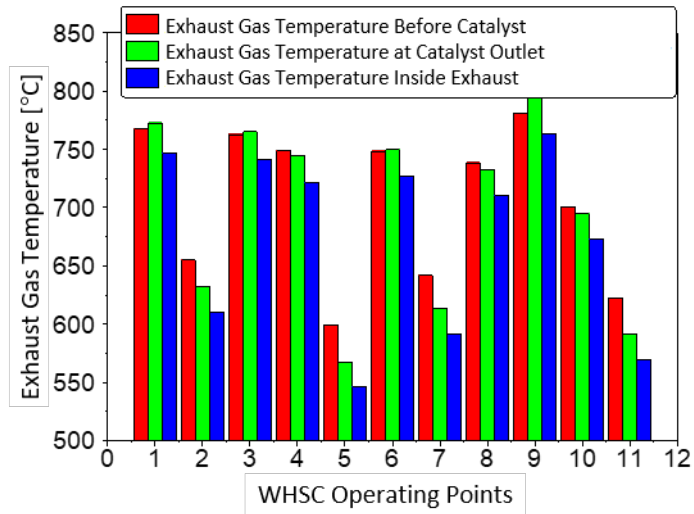


Figure 5-7 Simulation results for exhaust gas temperatures at different locations in the exhaust line of the Cursor 13 gas engine

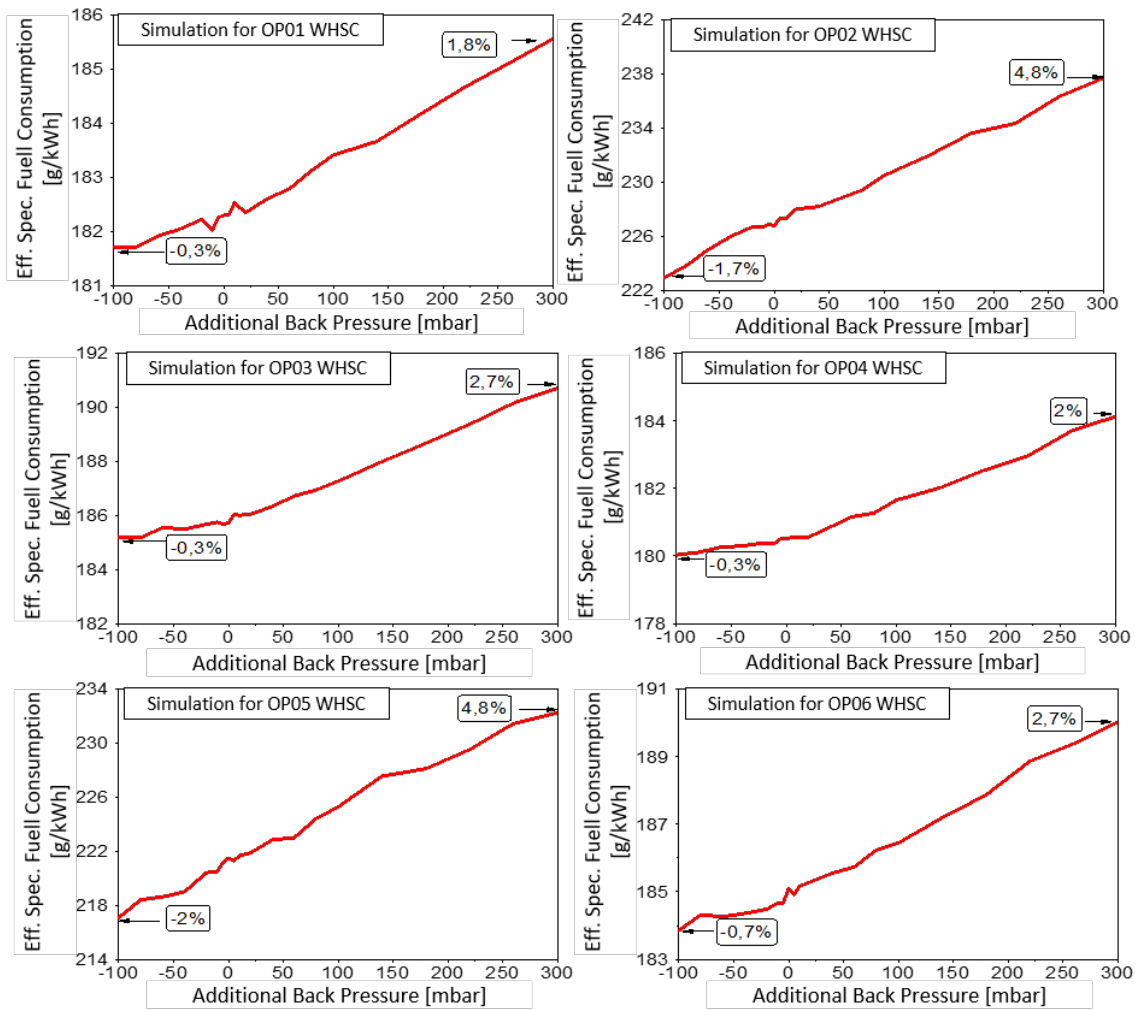


Figure 5-8 Simulative studies for the influence of additional exhaust gas backpressure on specific fuel consumption at WHSC operating points in OP01-06

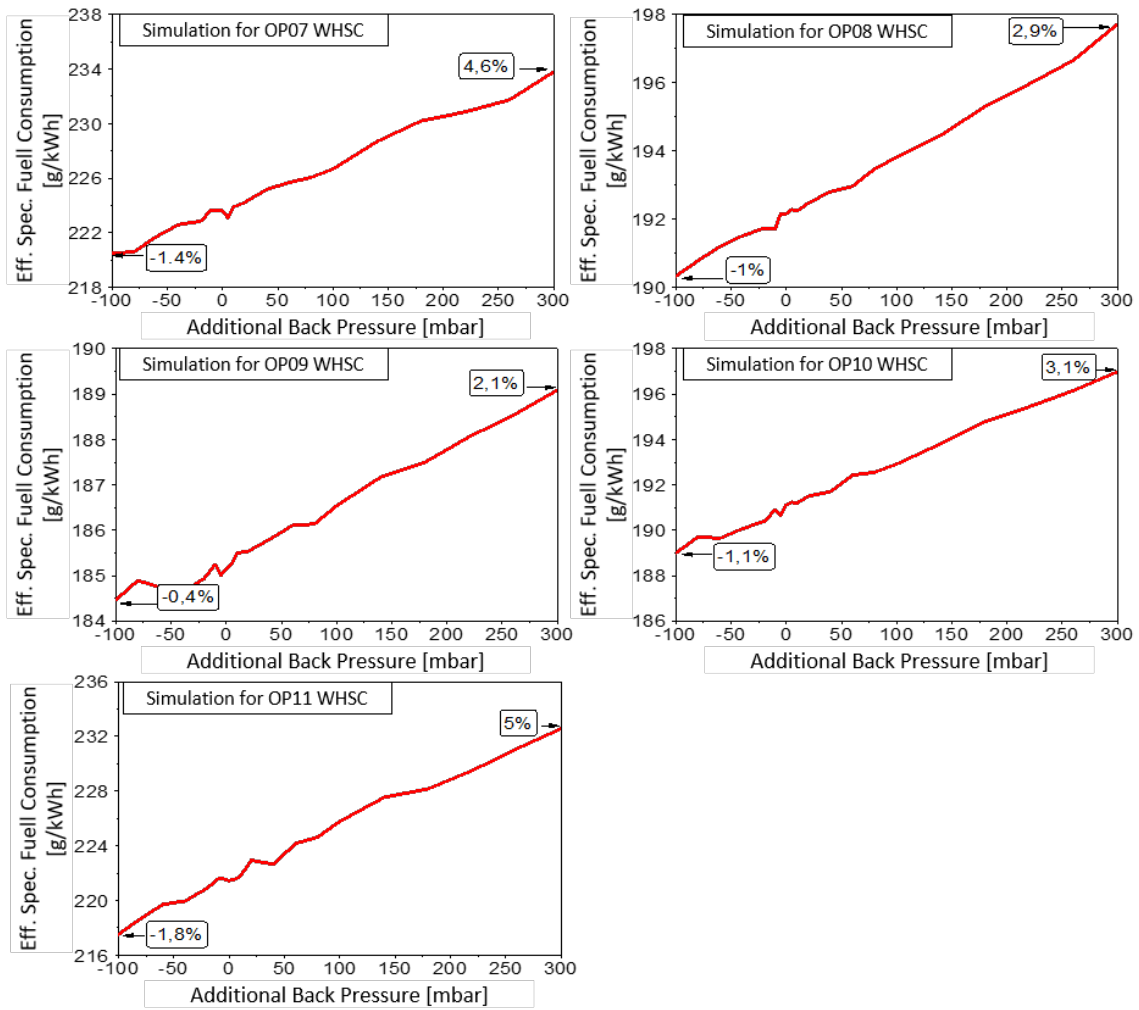


Figure 5-9 Continuation of Figure 5-8 for OP07-11

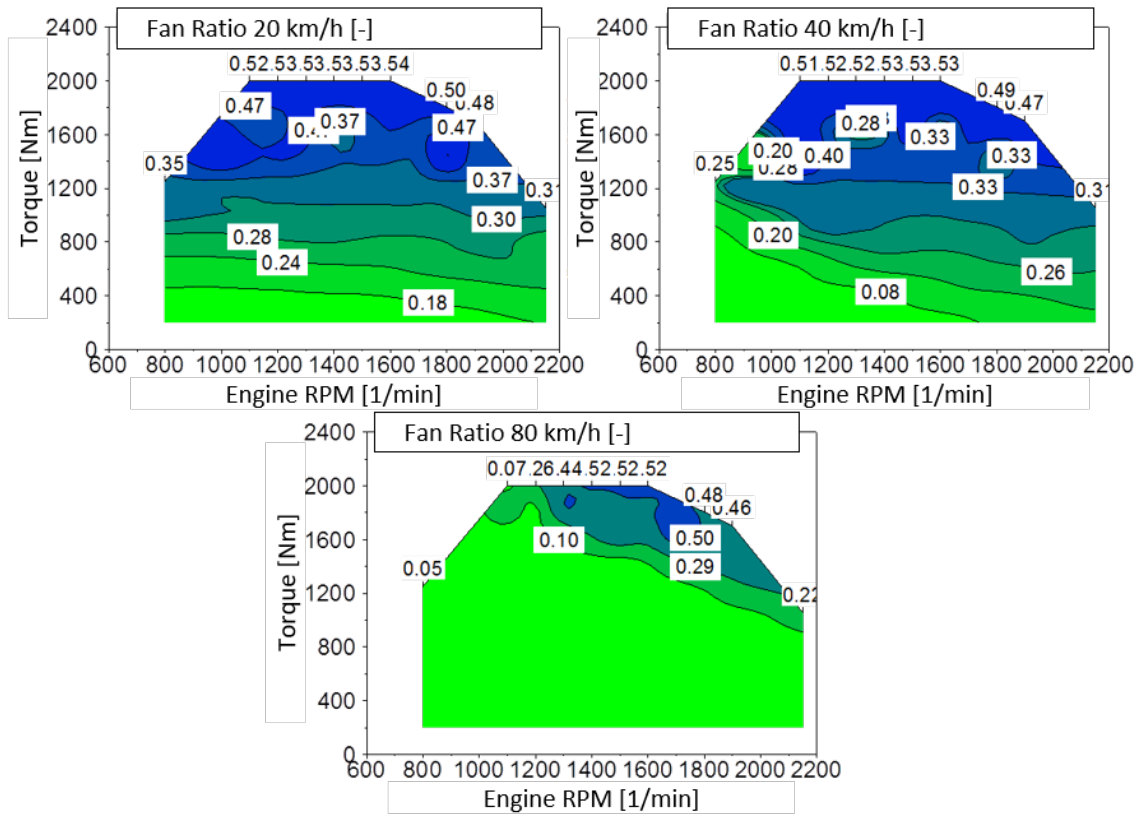


Figure 5-10 Fan ratios at the different driving speeds (ambient temperature of 20 °C; dry – 0 % humidity, air pressure of 1.013 bar)

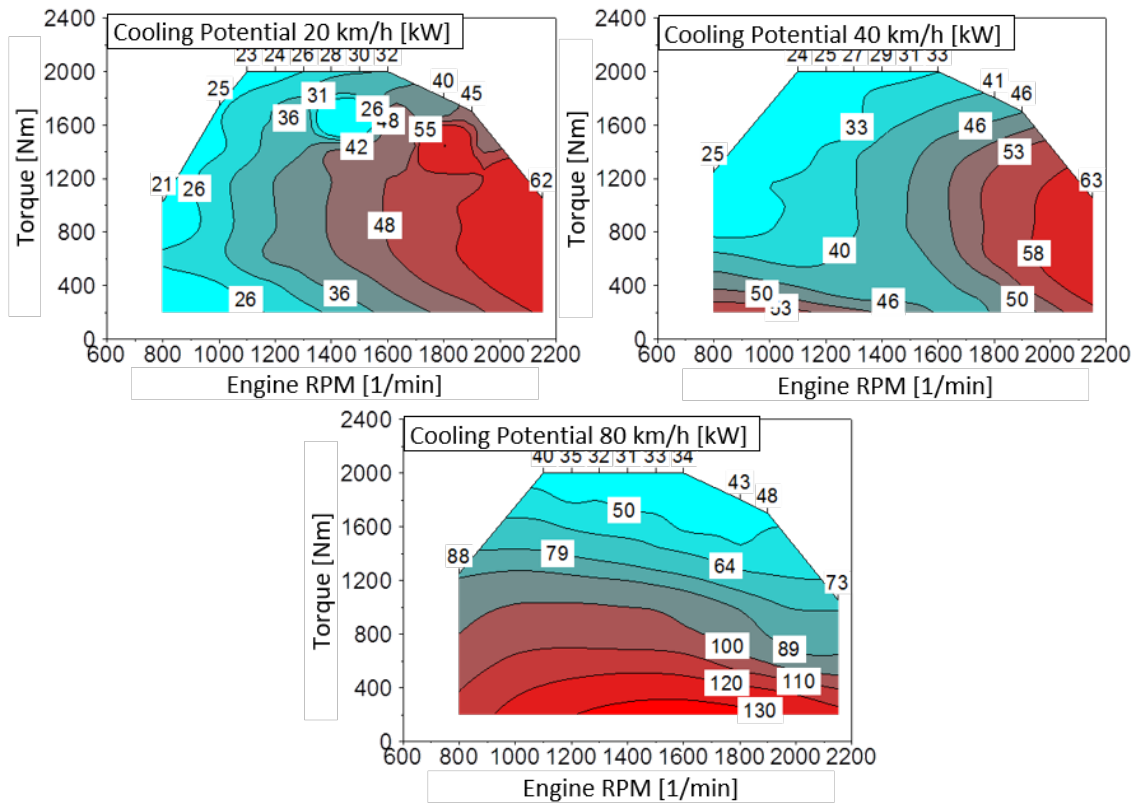


Figure 5-11 Simulation results for cooling potentials of the cooling system when the TEG is connected after the HT cooler with coolant temperature at the engine outlet of 100 °C as the target value at the different driving speeds under ambient temperature of 20 °C

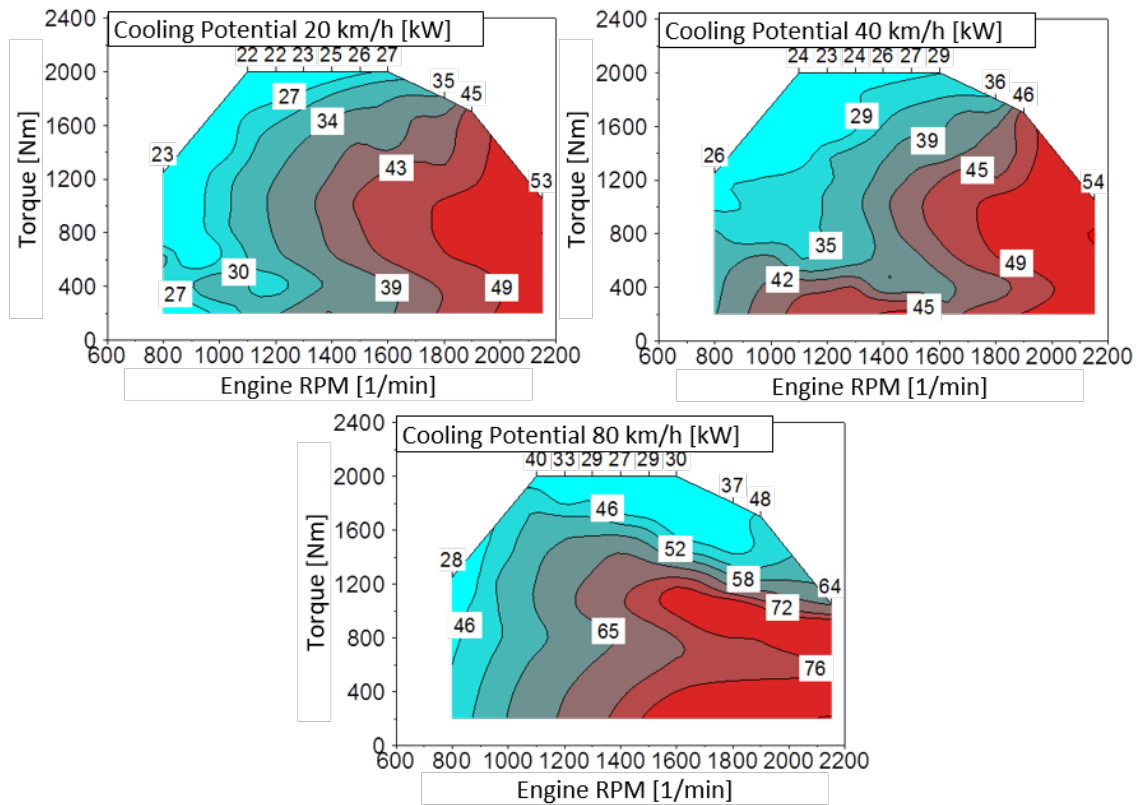


Figure 5-12 Simulation results for cooling potentials of the cooling system when the TEG is connected after the intercooler with coolant temperature at the engine outlet of 100 °C as the target value at the different driving speeds under ambient temperature of 20 °C

Table 5-3 HDV data for the simulation

Information/Parameter	Unit	Values
Gearbox	[-]	ZF 12 AS 2330 TD
Tires	[-]	315/80 R22.5
Flow resistance coefficient	[-]	0.6
Rolling resistance coefficient	[-]	0.01
Face	[m ²]	7.12
Vehicle mass with payload	[kg]	40 000

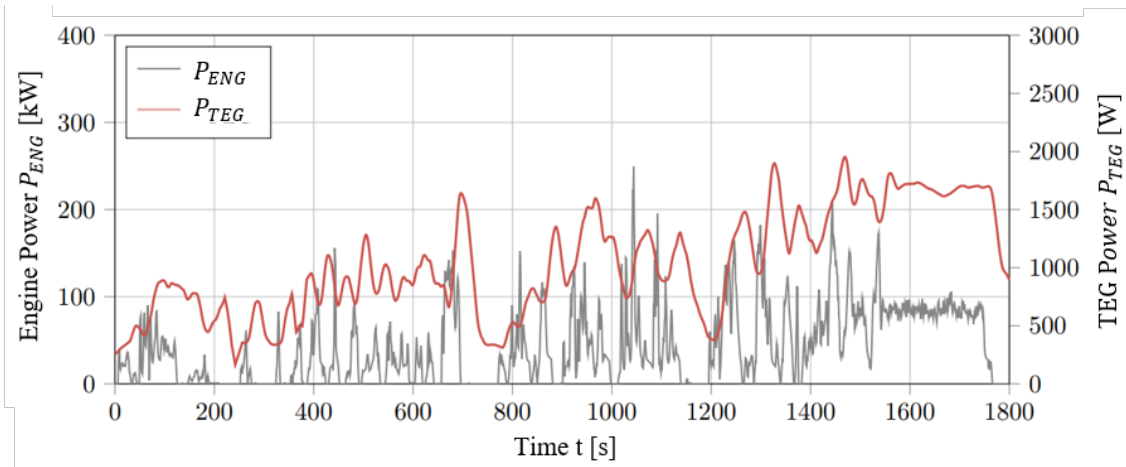


Figure 5-13 Result of the TEG performance in WHVC with 15 t TW in the result design with target for minimum TCO (TEG system integrated at the outlet of the EGA and in the LT CC)

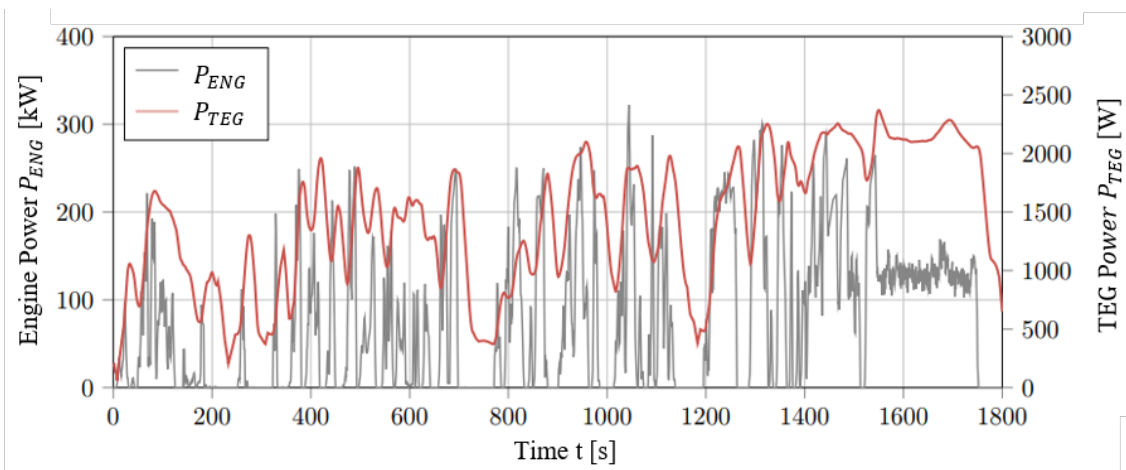


Figure 5-14 Result of the TEG performance in WHVC with 40 t TW in the result design with target for minimum TCO (TEG system integrated at the outlet of the EGA and in the LT CC)

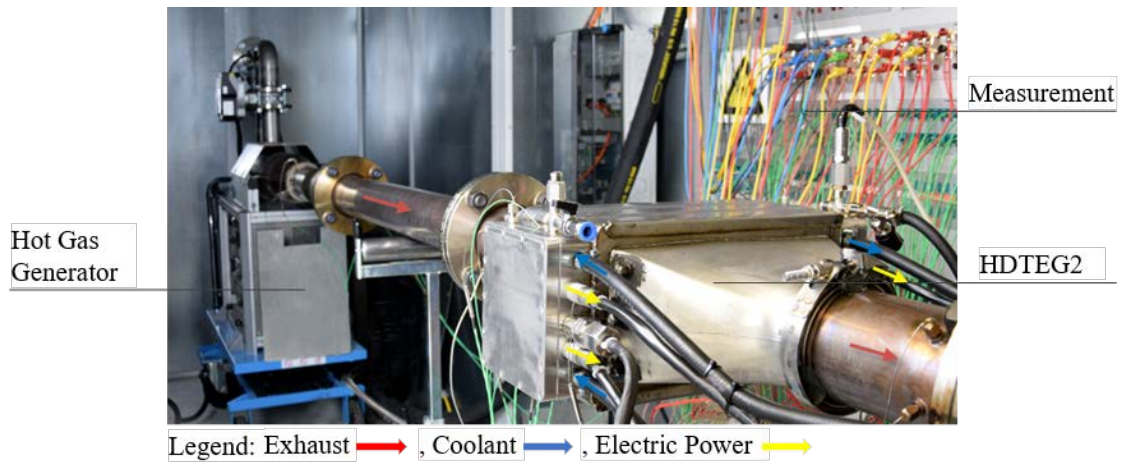


Figure 5-15 HDTEG2 functional model on DLR's own hot gas test rig

Table 5-4 Comparison of the hot gas backpressure Δp_{TEG} between the simulation and the experiments of the HDTEG1 and HDTEG2 functional models on the hot gas test rig

OP*		1.1	1.2	2.1	2.2	3.1	3.2
Designation	Unit	WHVC _{15 t,m}	WHVC _{15 t,max}	WHVC _{40 t,m}	WHVC _{40 t,max}	SHHS _{40 t,m}	SHHS _{40 t,max}
Simulation	[mbar]	2.1	11.9	6.1	19.7	10	26.7
HDTEG1	[mbar]	2.3	12.7	6	21	10.4	25.9
HDTEG2	[mbar]	2.1	13.4	6.5	22.6	10.6	28.7
Min. deviation	[%]	-3.1	7.2	-0.2	6.6	5.7	-2.9

*Between experiments, the boundary conditions vary in the range of max. $\mp 1.5\%$. The measurement deviation is not indicated for better clarity of the results.